# 2D and 3D Mapping Techniques

**Jean-Luc Starck**

*CEA, IRFU, AIM, Service d'Astrophysique, France*

http://jstarck.cosmostat.org

**Collaborators:**

Francois Lanusse, Adrienne Leonard, Austin Peel, Sandrine Pires




# Map Making: ILL Posed Inverse Problem

Y = H X + N

Need to add constraint

$$min_X = \| Y - HX \|^2 \quad s.t. \;\; \mathcal{C}(X, H)$$

# Map Making: ILL Posed Inverse Problem

Y = H X + N

Need to add constraint

$$min_X = \| Y - HX \|^2 \quad s.t. \;\; \mathcal{C}(X, H)$$

Or blind ill posed problems

$$min_{H,X} = \| Y - HX \|^2 \quad s.t. \;\; \mathcal{C}(X, H)$$

**- Part I: 2D and 3D WL Mass Maps**

- Part II: CMB Map Recovery

- Part III: Radio-Interferometry Image Reconstruction

# Convergence Map

- **Mass Mapping**:
  - Originally, mass maps were considered not scientifically useful, but the situation is now clearly different.
  - The field is evolving, and several 2D and 3D codes now exist.
  - Science case work ongoing, and most requirements are not defined

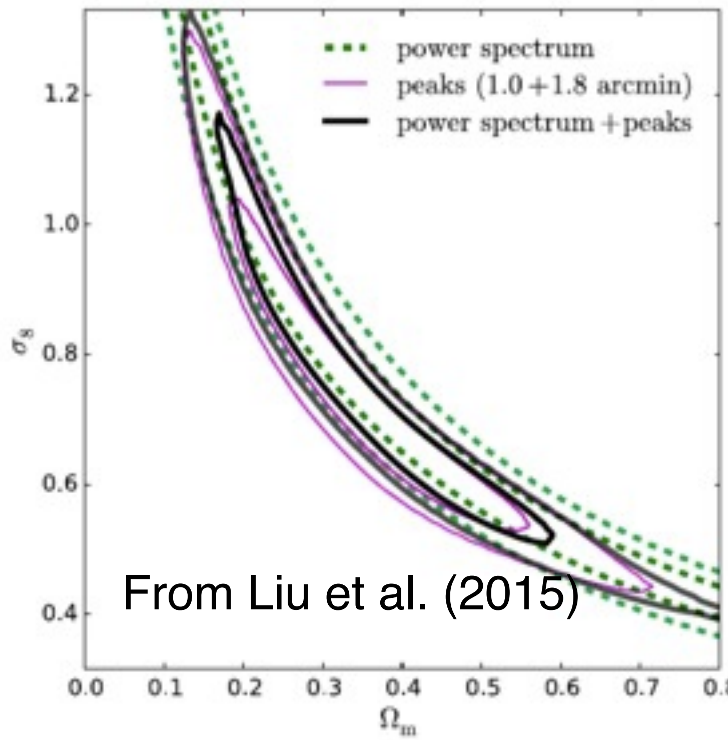


Cosmo. Parameters


Clusters

$$\hat{\kappa} = P_1 \hat{\gamma}_1 + P_2 \hat{\gamma}_2$$

$$P_1(k) = \frac{k_1^2 - k_2^2}{k^2}$$

$$P_2(k) = \frac{2k_1 k_2}{k^2}$$

# 2D Mass Mapping Problems

•**Missing data** (mask and limited number densities):

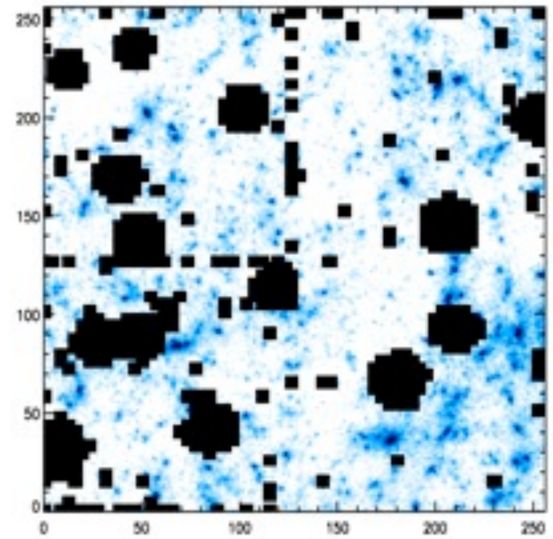


•**Shape noise:**

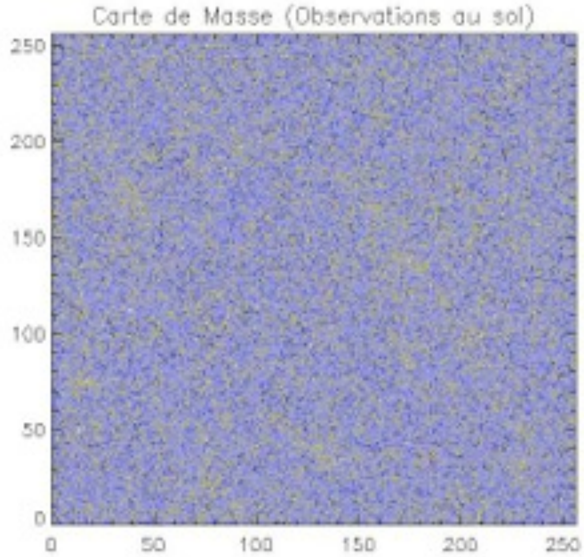


•**Reduced shear:** $$g = \frac{\gamma}{1-\kappa}$$

the observed reduced shear is invariant under the transformation: $\kappa^{'} = \lambda\kappa(1-\lambda)$

**=> Mass-sheet degeneracy problem**

# Handling Missing Data (no noise): Binning+Smoothing

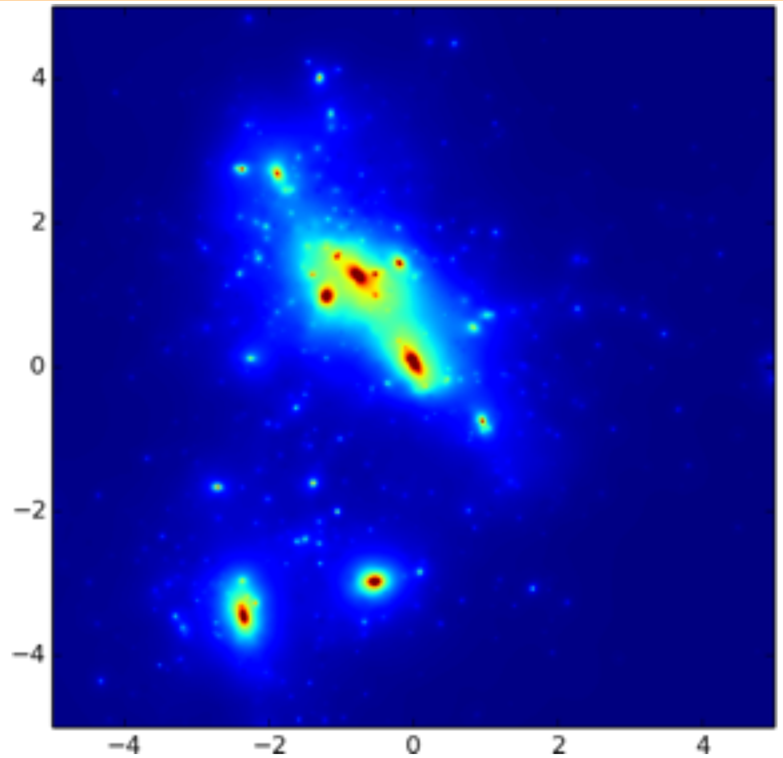

Input

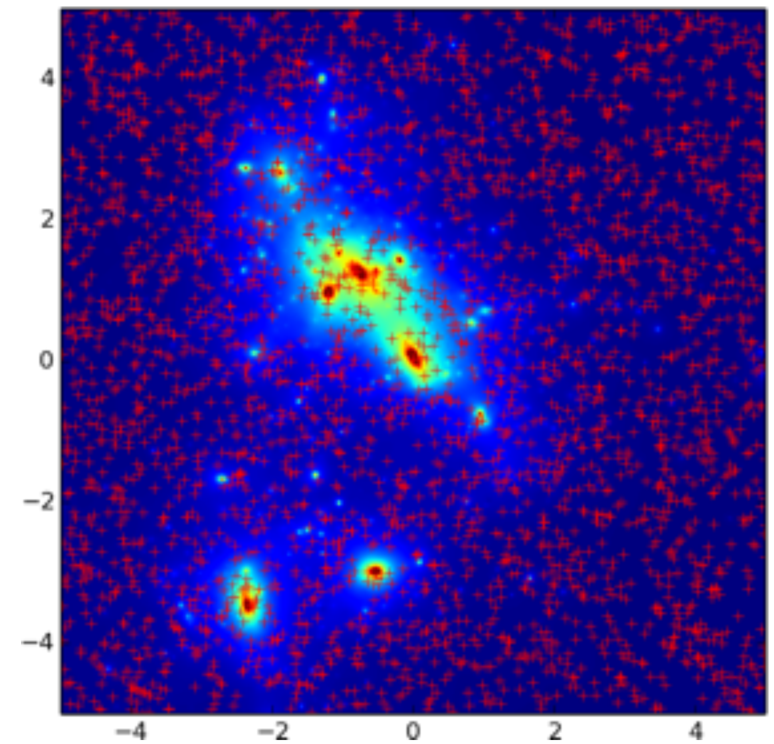

Galaxy catalogue with 30 gal/arcmin$^2$

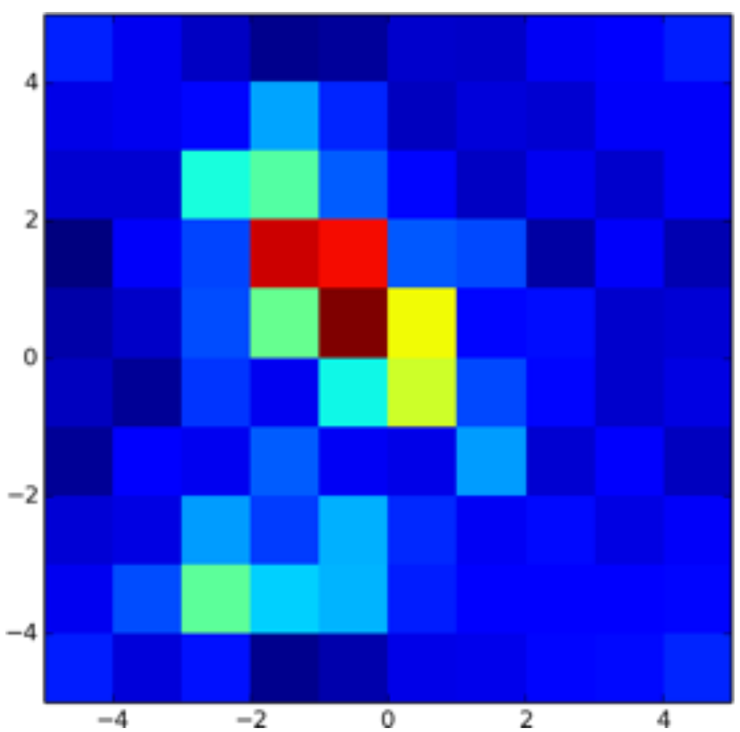

Kaiser-Squires with 1' bins

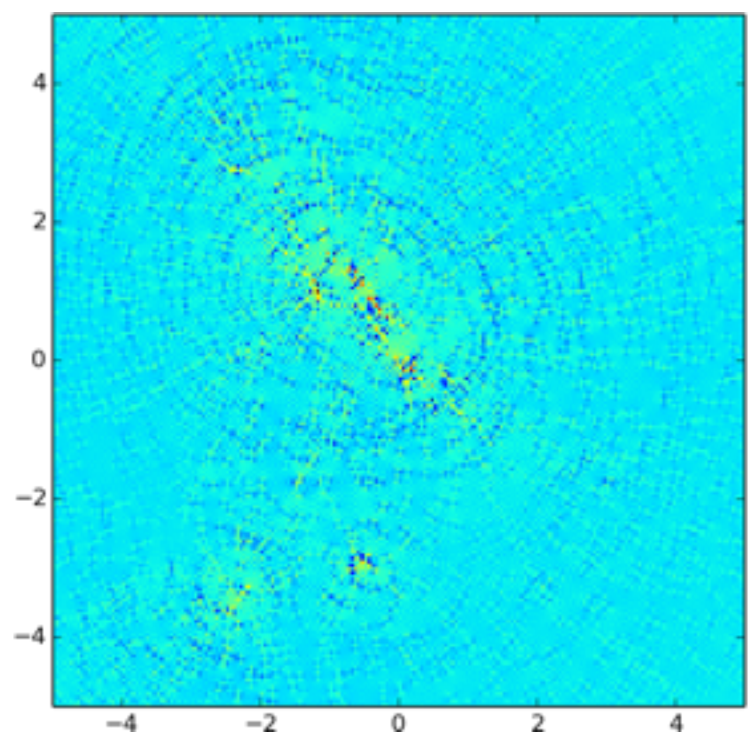

Kaiser-Squires with 0.05' bins

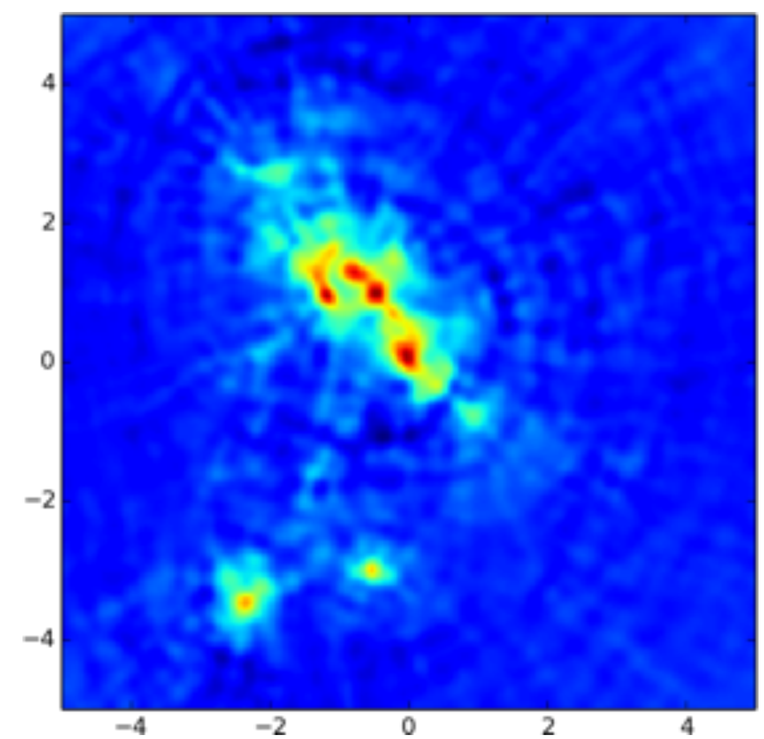

KS with 0.05' bins + 0.1’ smoothing

# Mass mapping as an inverse problem

Binned data: $\gamma = F^* P F \kappa$

Unbinned data: $\gamma = T^* P F \kappa$

T = Non Equispaced Discrete Fourier Transform (NDFT)

$$\boxed{\min_{\kappa} \frac{1}{2} \parallel \gamma - \mathbf{P}\kappa \parallel_2^2 \quad \text{with} \quad \mathbf{P} = T^* P F}$$

$$g = \frac{\gamma}{1-\kappa} \longrightarrow \boxed{\min_{\kappa} \frac{1}{2} \parallel (1-\kappa) g - \mathbf{P}\kappa \parallel_2^2}$$

$\mathbf{P} = T^* P F$ is not directly invertible $\Rightarrow$ **Linear inverse problem**.

# Mass mapping as an inverse problem

Binned data: $\gamma = F^* P F \kappa$

Unbinned data: $\gamma = T^* P F \kappa$

T = Non Equispaced Discrete Fourier Transform (NDFT)

$$\boxed{\min_{\kappa} \frac{1}{2} \parallel \gamma - \mathbf{P}\kappa \parallel_2^2 \quad \text{with} \quad \mathbf{P} = T^* P F}$$

$$g = \frac{\gamma}{1-\kappa} \longrightarrow \boxed{\min_{\kappa} \frac{1}{2} \parallel (1-\kappa)g - \mathbf{P}\kappa \parallel_2^2 + \mathcal{C}(\kappa)}$$

$\mathbf{P} = T^* P F$ is not directly invertible $\Rightarrow$ **Linear inverse problem.**

# Wavelet Aperture Mass (WAM)

$$M_{ap}(\boldsymbol{\theta}) = \int d^2\boldsymbol{\vartheta}\ \gamma_t(\boldsymbol{\vartheta})Q(|\boldsymbol{\vartheta}|)$$

$$\boxed{M_{ap}(\theta) = (\boldsymbol{\Phi}^t\kappa)_\theta}$$

$\Rightarrow$ Wavelets filters are formally **indentical** to Mass aperture

A. Leonard, S. Pires, J.-L. Starck, "Fast Calculation of the Weak Lensing Aperture Mass Statistic", **MNRAS**, 423, pp 3405-3412, 2012.

but wavelets presents many advantages:
- compensated and **compact** support filters
- **fast** calculation:
- **all scales** processed in one step.
- **reconstruction** is possible
  ==> image restoration for peak counting

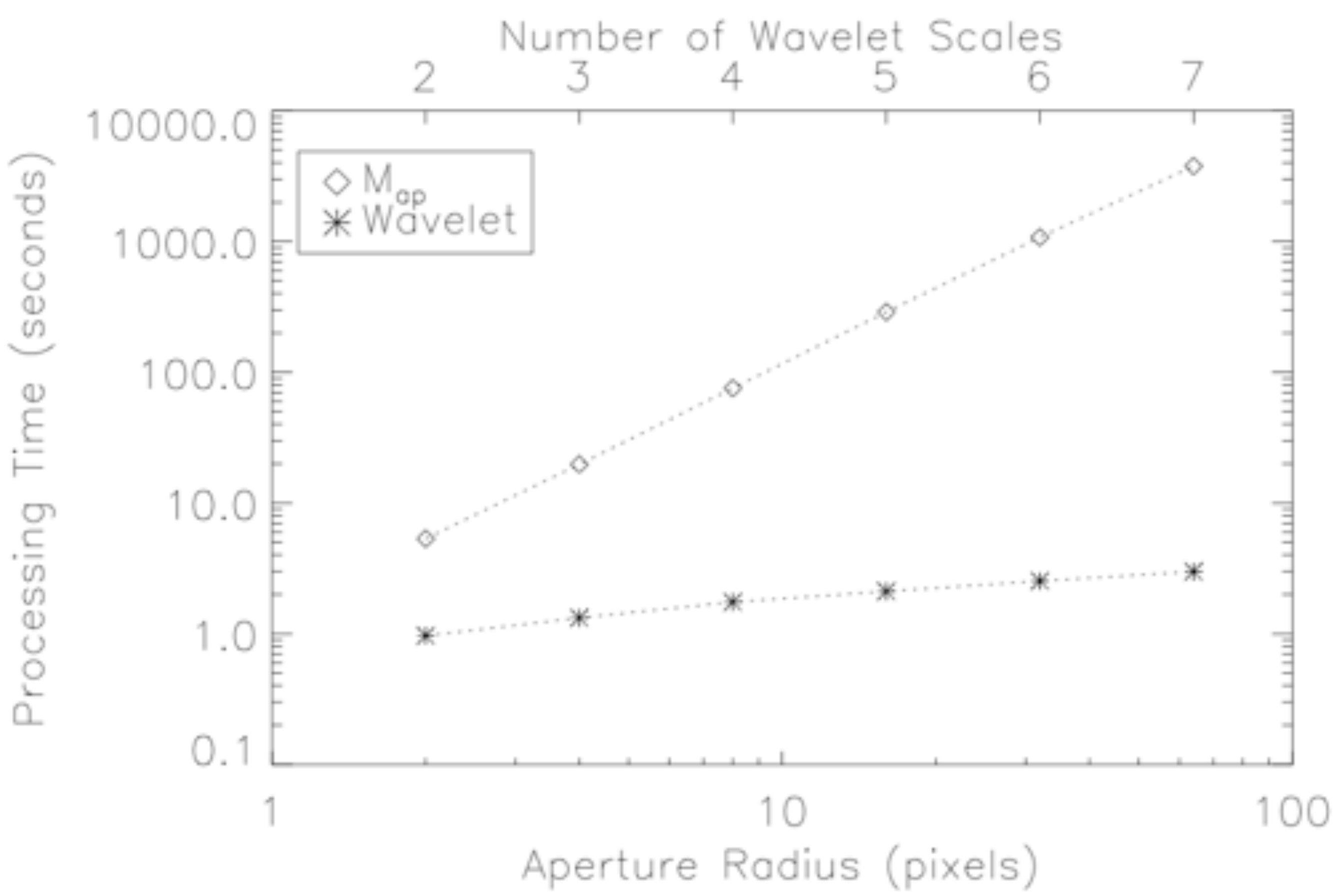

# Wavelet Aperture Mass (WAM)

$$\boxed{M_{ap}(\theta) = (\mathbf{\Phi}^t \kappa)_\theta}$$

$$\mathbf{\Phi}^t \kappa = \alpha = \{\alpha_1, \ldots, \alpha_J\}$$

The matrix $\mathbf{\Phi}$ corresponds to the representation space, it is also called the dictionary.

# Mass mapping as an inverse problem

Unbinned data: $\gamma = T^* P F \kappa$

T = Non Equispaced Discrete Fourier Transform (NDFT)

$$\min_{\kappa} \frac{1}{2} \parallel \gamma - \mathbf{P}\kappa \parallel_2^2 + \mathcal{C}(\kappa)$$ with $\mathbf{P} = T^* P F$

$$M_{ap}(\theta) = (\mathbf{\Phi}^t \kappa)_\theta$$

=> A ***multi-scale peak counting prior*** **(WAM Constraint)**

$$\boxed{\mathcal{C}(\kappa) = \sum_{\theta} \parallel (\Phi^t \kappa)_\theta \parallel_p = \sum_j \parallel \alpha_j \parallel_p}$$

$$\mathcal{C}(\kappa) = \sum_{\theta} \parallel (\Phi^t \kappa)_\theta \parallel_1 = \parallel \Phi^t \kappa \parallel_1$$

$$\|X\|_p = (\sum_i \mid X_i \mid^p)^{\frac{1}{p}}$$

$$\|X\|_1 = \sum_i \mid X_i \mid$$

# L1 Norm & Sparsity

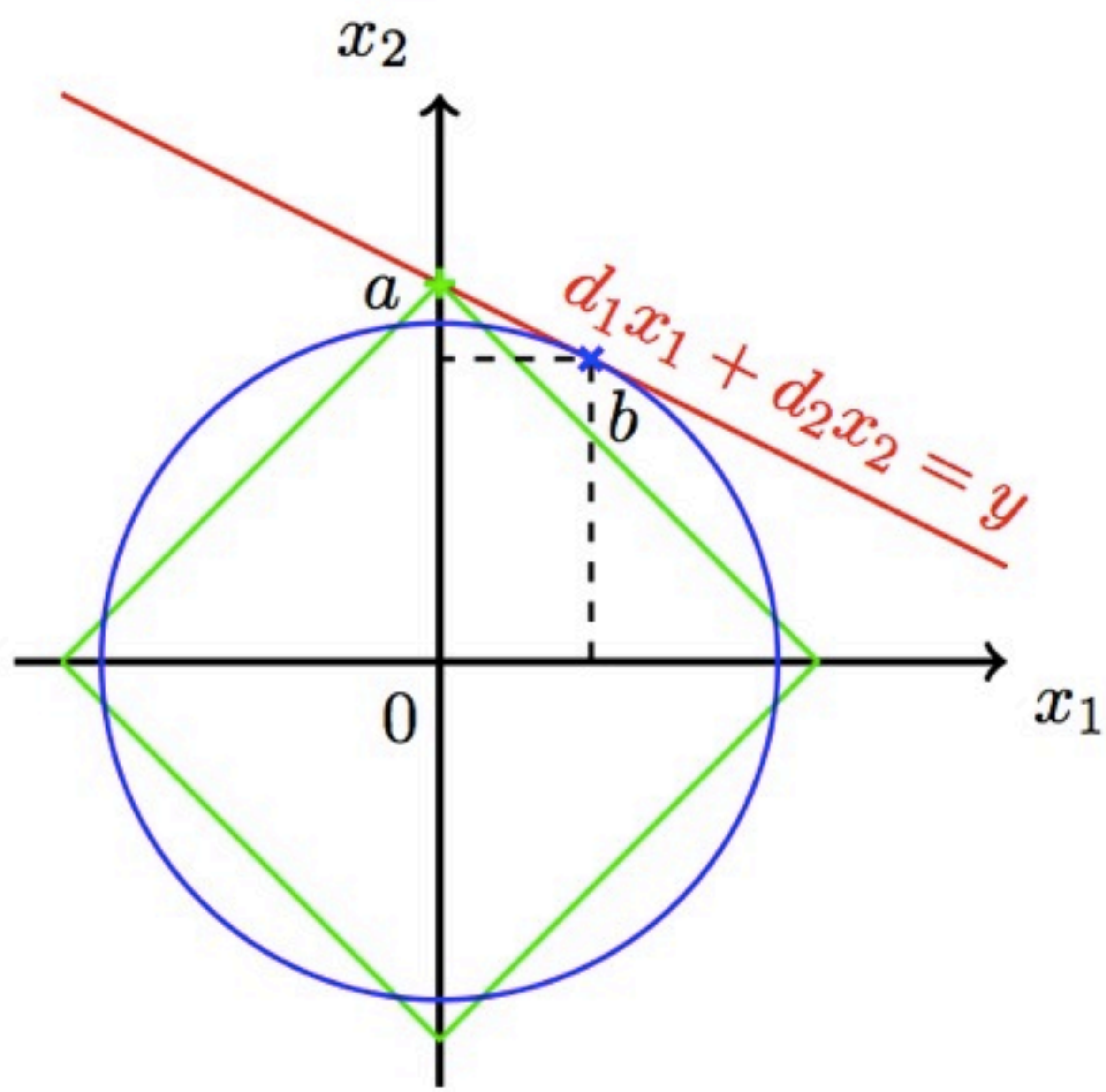


$$\mathcal{C}(\kappa) = \| \Phi^t \kappa \|_1$$

# Sparse Recovery & Inverse Problems

$$Y = HX + N$$

$X = \Phi\alpha$, and $\alpha$ is sparse

- Denoising
- Deconvolution
- Component Separation
- Inpainting
- Blind Source Separation
- Minimization algorithms
- Compressed Sensing

$$\min_{\alpha} \|\alpha\|_p^p \quad \text{subject to} \quad \|Y - H\Phi\alpha\|^2 \leq \epsilon$$

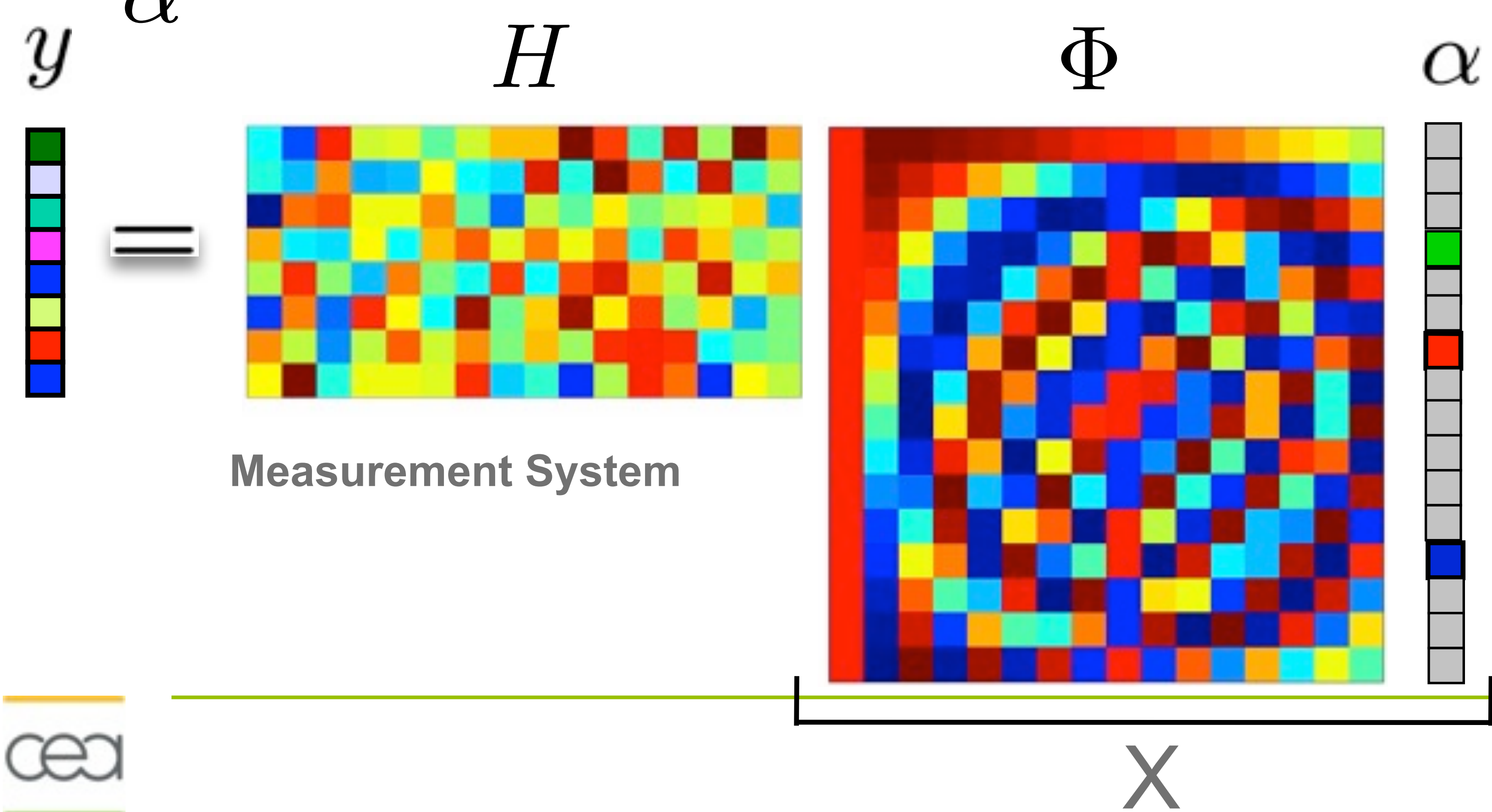


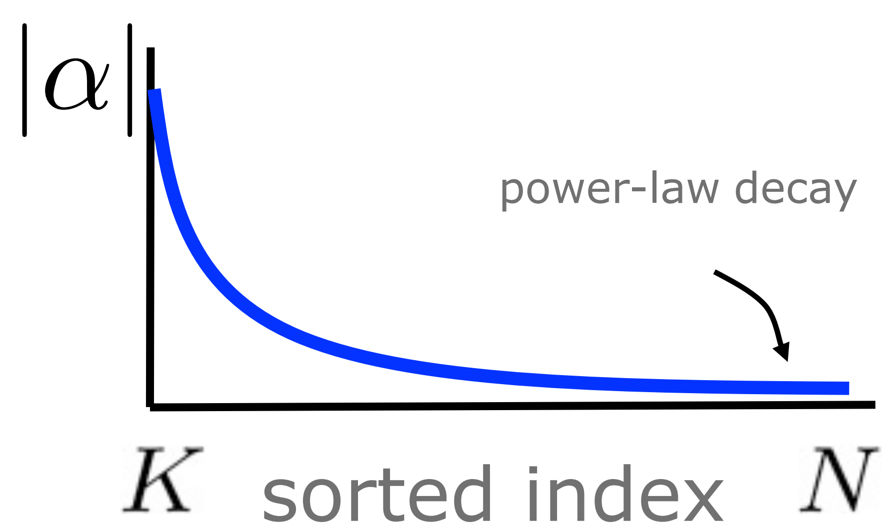

# Sparsity and Mass mapping

Mass-Shear: $\gamma = \mathbf{P}\kappa$ with $\mathbf{P} = T^* P F$

T = Non Equispaced Discrete Fourier Transform (NDFT)

$$\min_{\kappa} \frac{1}{2} \parallel \gamma - \mathbf{P}\kappa \parallel_2^2$$

sparse regularizaton

$$\boxed{\min_{\kappa} \frac{1}{2} \parallel \gamma - \mathbf{P}\kappa \parallel_2^2 + \lambda \parallel \mathbf{\Phi}^t \kappa \parallel_1}$$

$$g = \frac{\gamma}{1-\kappa} \longrightarrow \boxed{\min_{\kappa} \frac{1}{2} \parallel (1-\kappa) g - \mathbf{P}\kappa \parallel_2^2 + \lambda \parallel \mathbf{\Phi}^t \kappa \parallel_1}$$

=> Write the mass-mapping as a single optimization problem with a ***multi-scale sparsity prior*** addressing many issues (i.e. reduced shear, missing data, noise).

F. Lanusse, J.-L. Starck, A. Leonard, and S. Pires, High Resolution Weak Lensing Mass Mapping combining Shear and Flexion, submitted.

# Flexion + Redshift Information

We can integrate flexion in our reconstruction framework

=> **Jointly** fit shear and flexion

$$\min_{\kappa} \frac{1}{2} \parallel (1-\kappa) \begin{bmatrix} g \\ F \end{bmatrix} - \begin{bmatrix} \mathbf{P} \\ \mathbf{Q} \end{bmatrix} \kappa \parallel_2^2 + \lambda \parallel \mathbf{\Phi}^t \kappa \parallel_1$$

=> **Jointly** fit shear and flexion with redshift information

$$\min_{\kappa} \frac{1}{2} \parallel (1-\mathbf{Z}\kappa) \begin{bmatrix} g \\ F \end{bmatrix} - \mathbf{Z} \begin{bmatrix} \mathbf{P} \\ \mathbf{Q} \end{bmatrix} \kappa \parallel_2^2 + \lambda \parallel \mathbf{\Phi}^t \kappa \parallel_1$$

with $\mathbf{Z} = \Sigma_{critic}^{\infty} / \Sigma_{critic}(z_i)$

$$\Sigma_{crit}^{\infty} = \lim_{z \to \infty} \Sigma_{crit}(z)$$

$$\Sigma_{crit}(z_s) = \frac{c^2}{4\pi G} \frac{D_S}{D_L D_{LS}}$$

Individual redshifts have two benefits:

•Directly map the **surface mass density** of the lens

•Mitigate the **mass-sheet degeneracy** when $\kappa$ becomes significant (Bradac, Lombard and Schneider, 2004)

# The 2D Glimpse Algorithm

$$\min_{\kappa} \frac{1}{2} F(\kappa) + \lambda \parallel \mathbf{\Phi}^t \kappa \parallel_1 \quad \text{with} \quad F(\kappa) = \frac{1}{2} \parallel (1-\kappa) g - \mathbf{P} \kappa \parallel_2^2$$

Primal-dual splitting:

$$\boxed{\begin{cases} \kappa^{(n+1)} & = & \kappa^{(n)} + \tau \left( \nabla F(\kappa^{(n)}) + \mathbf{\Phi} \alpha^{(n)} \right) \\ \alpha^{(n+1)} & = & (\mathrm{Id} - \mathrm{ST}_\lambda) \left( \alpha^{(n+1)} + \mathbf{\Phi}^t (2\kappa^{(n+1)} - \kappa^{(n)}) \right) \end{cases}}$$

Condat-Vu algorithm, 2013

A few remarks:
- Recovers the convergence from the reduced shear
- **P** can be defined with and without binning the shear
- **P** can be ill-posed in case of missing data
- Sparse regularization of noise and missing data
  We use isotropic wavelets, well adapted to the recovery of clusters.

- Fast and flexible algorithm
- Sparsity constraint $\lambda$ estimated locally by noise simulations $\Longrightarrow$ Accounts for **survey geometry**, **varying noise levels**

# Example with 93 % of missing data

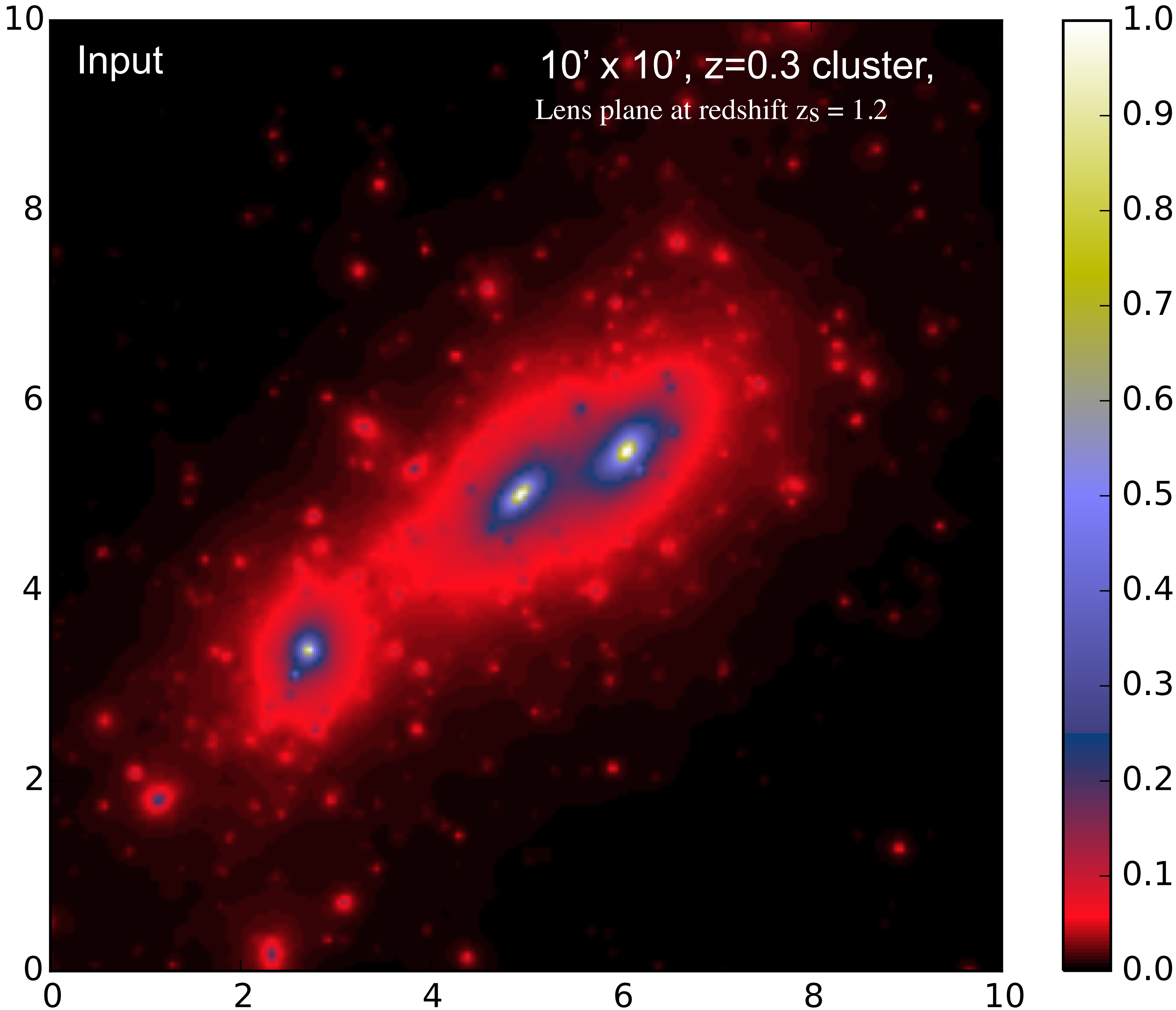


CosmoStat Lab

**Galaxy distribution: 93% of missing pixels**, corresponding to 30 galaxies per square arcminute

# Example with 93 % of missing data

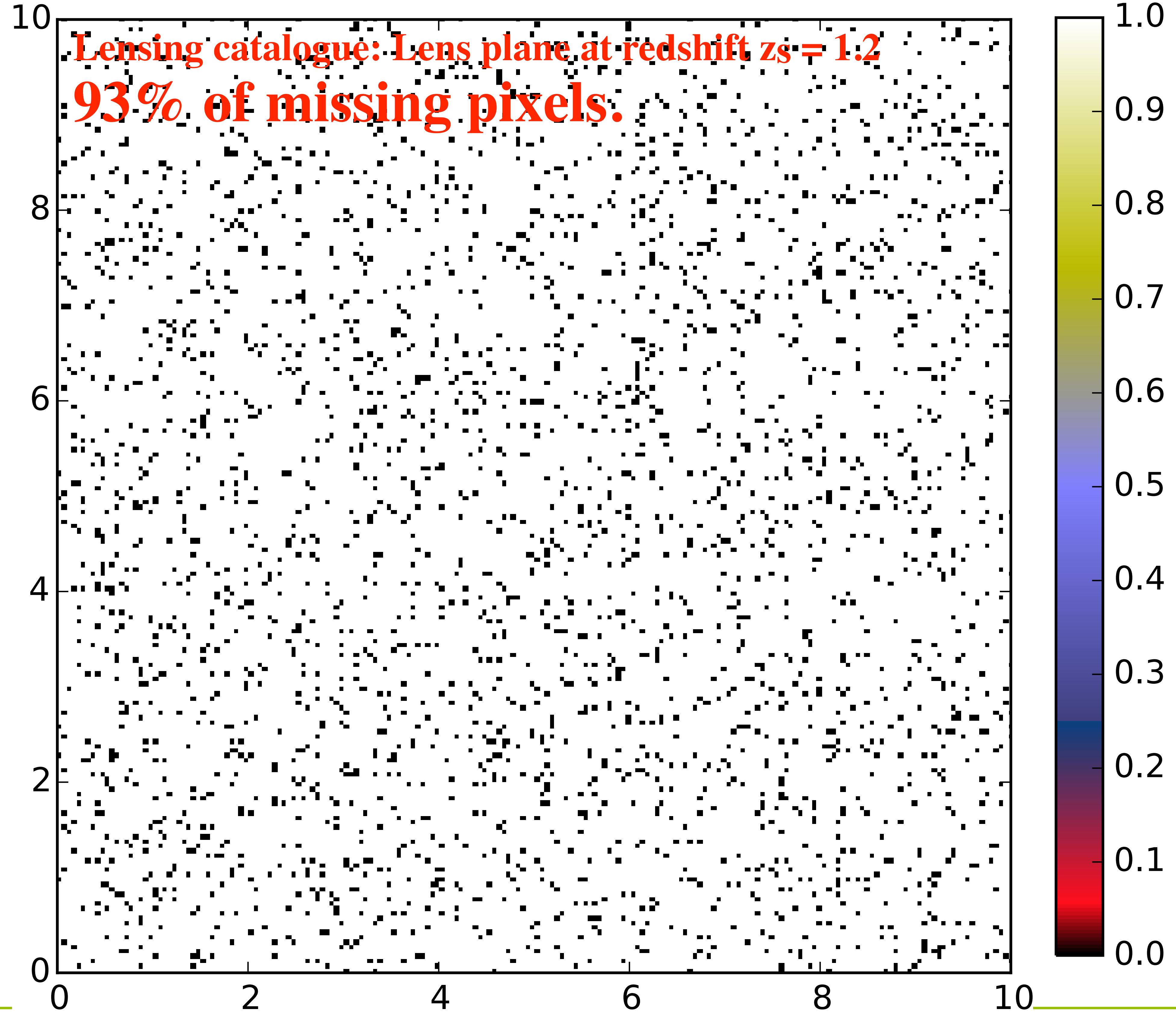


CosmoStat Lab

**Galaxy distribution: 93% of missing pixels**, corresponding to 30 galaxies per square arcminute

# Example with 93 % of missing data

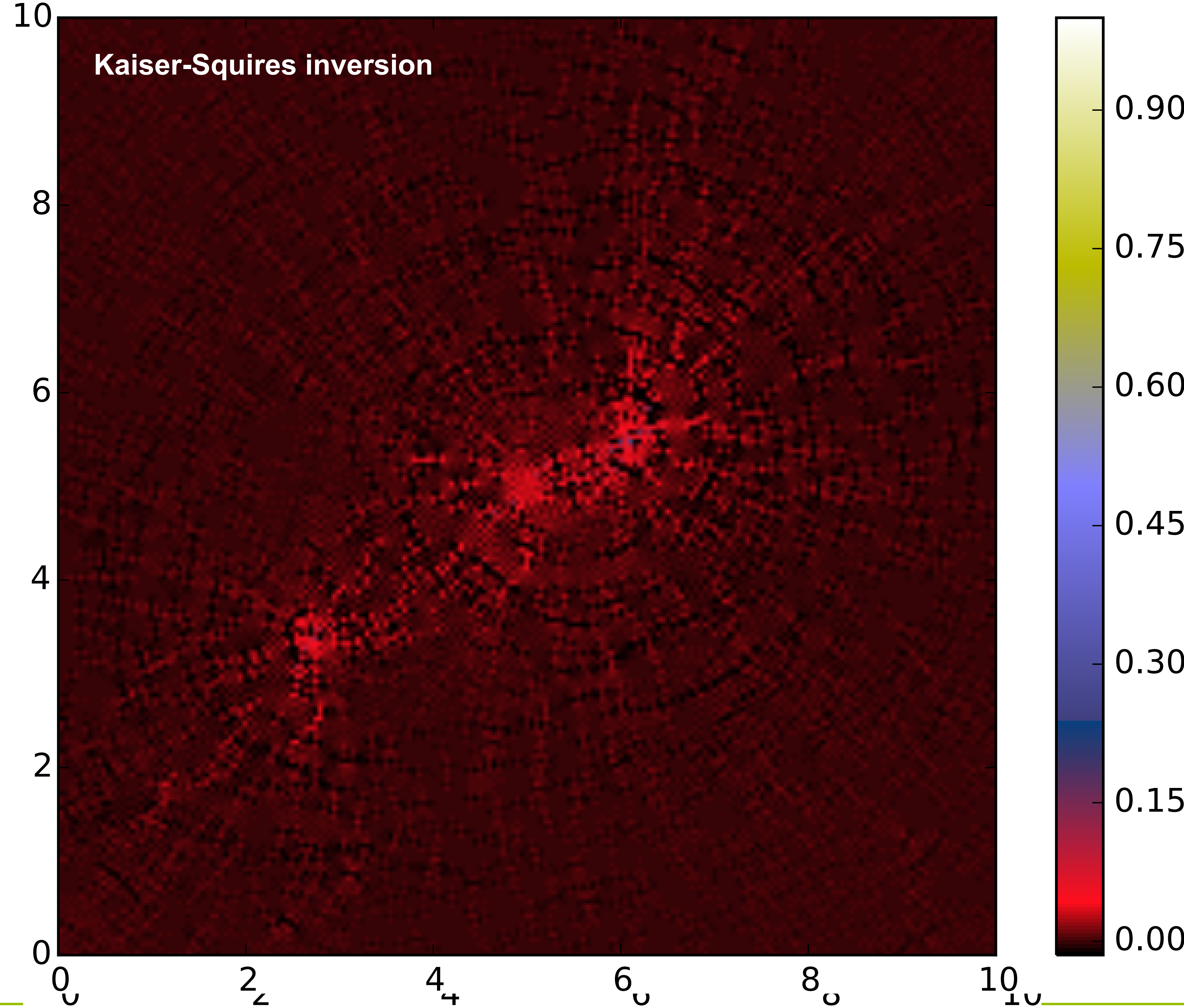


CosmoStat Lab

**Galaxy distribution:** **93% of missing pixels**, corresponding to 30 galaxies per square arcminute

# Example with 93 % of missing data

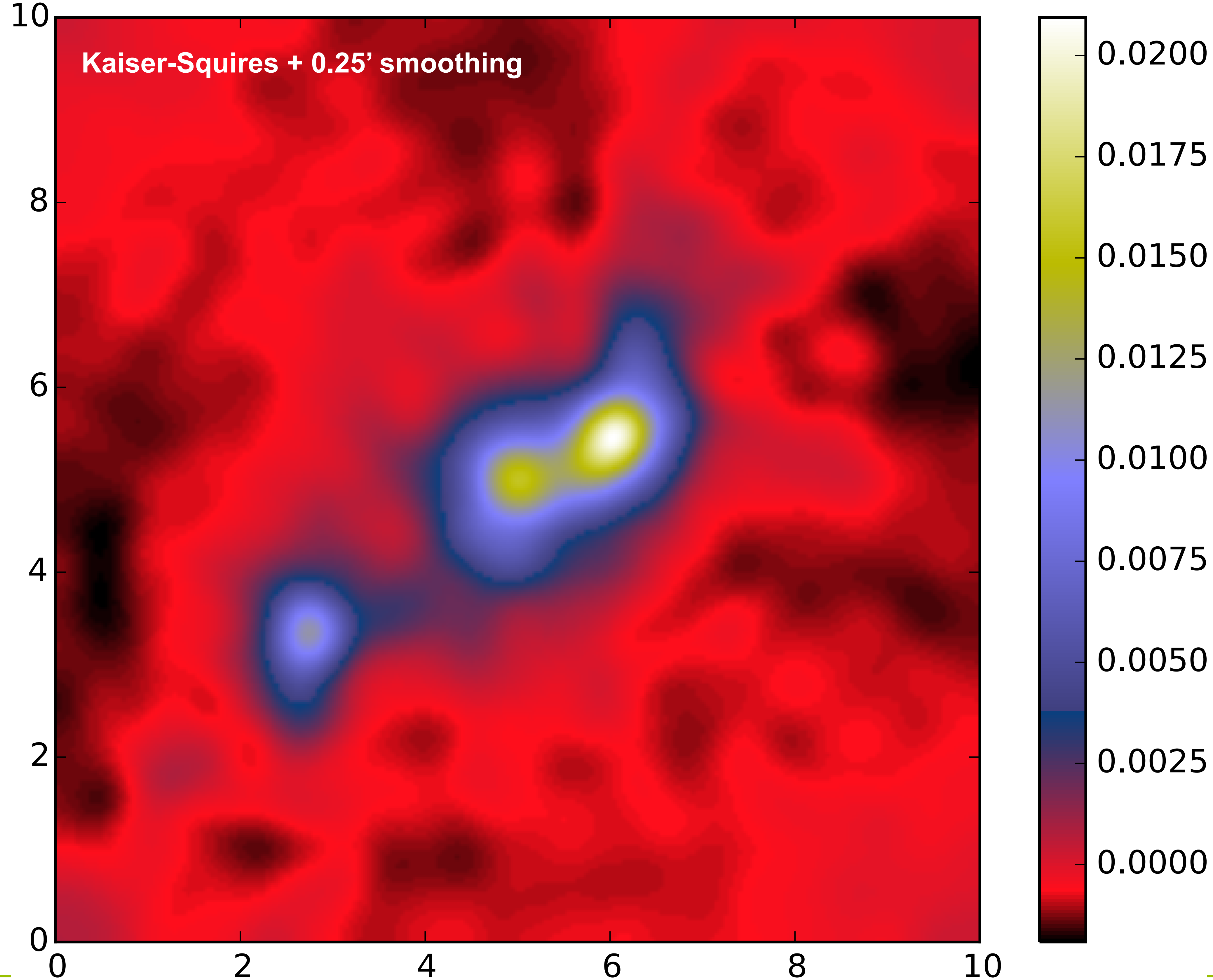


CosmoStat Lab

**Galaxy distribution: 93% of missing pixels**, corresponding to 30 galaxies per square arcminute

# Example with 93 % of missing data

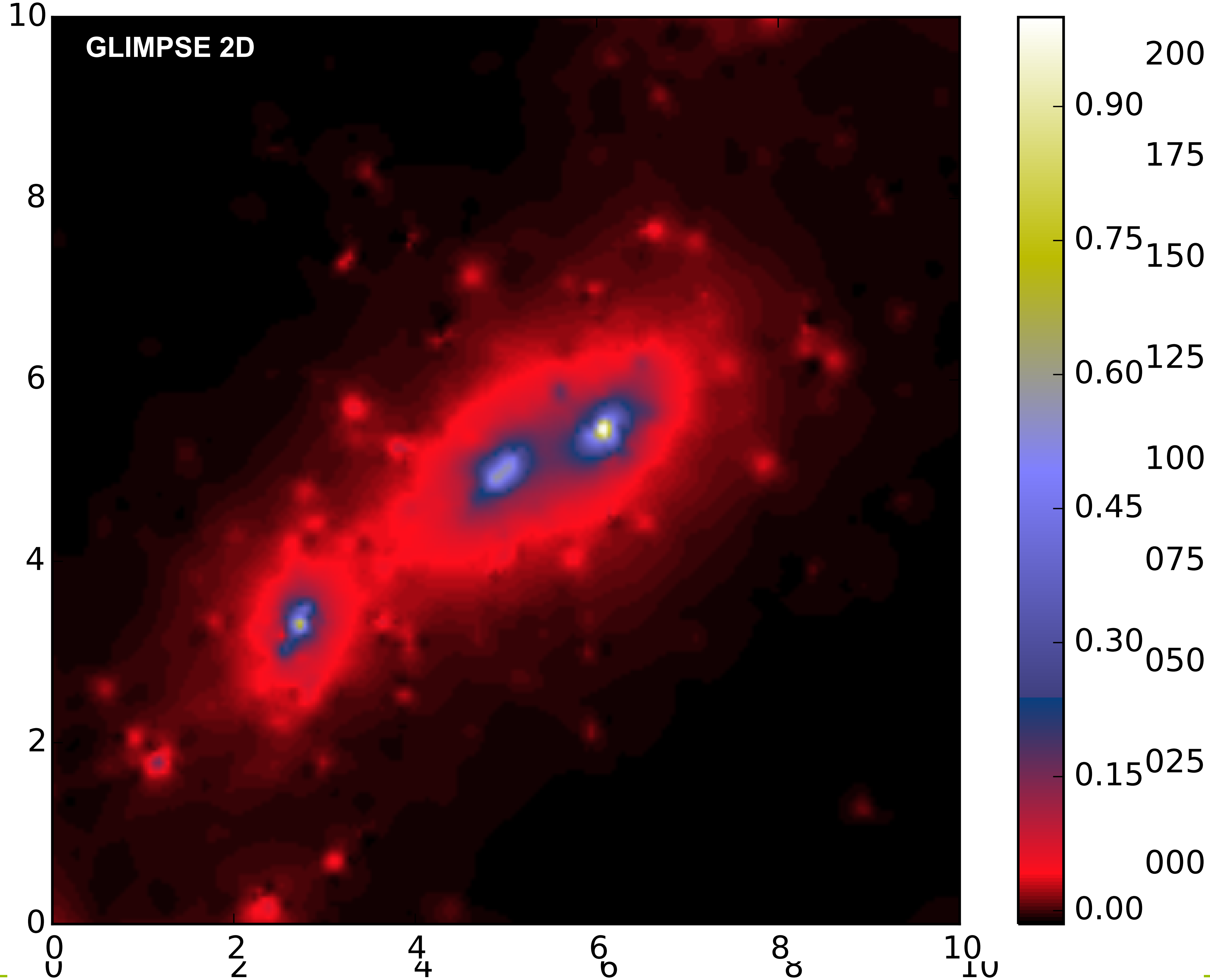


CosmoStat Lab

**Galaxy distribution:** **93% of missing pixels**, corresponding to 30 galaxies per square arcminute

# Example with 93 % of missing data

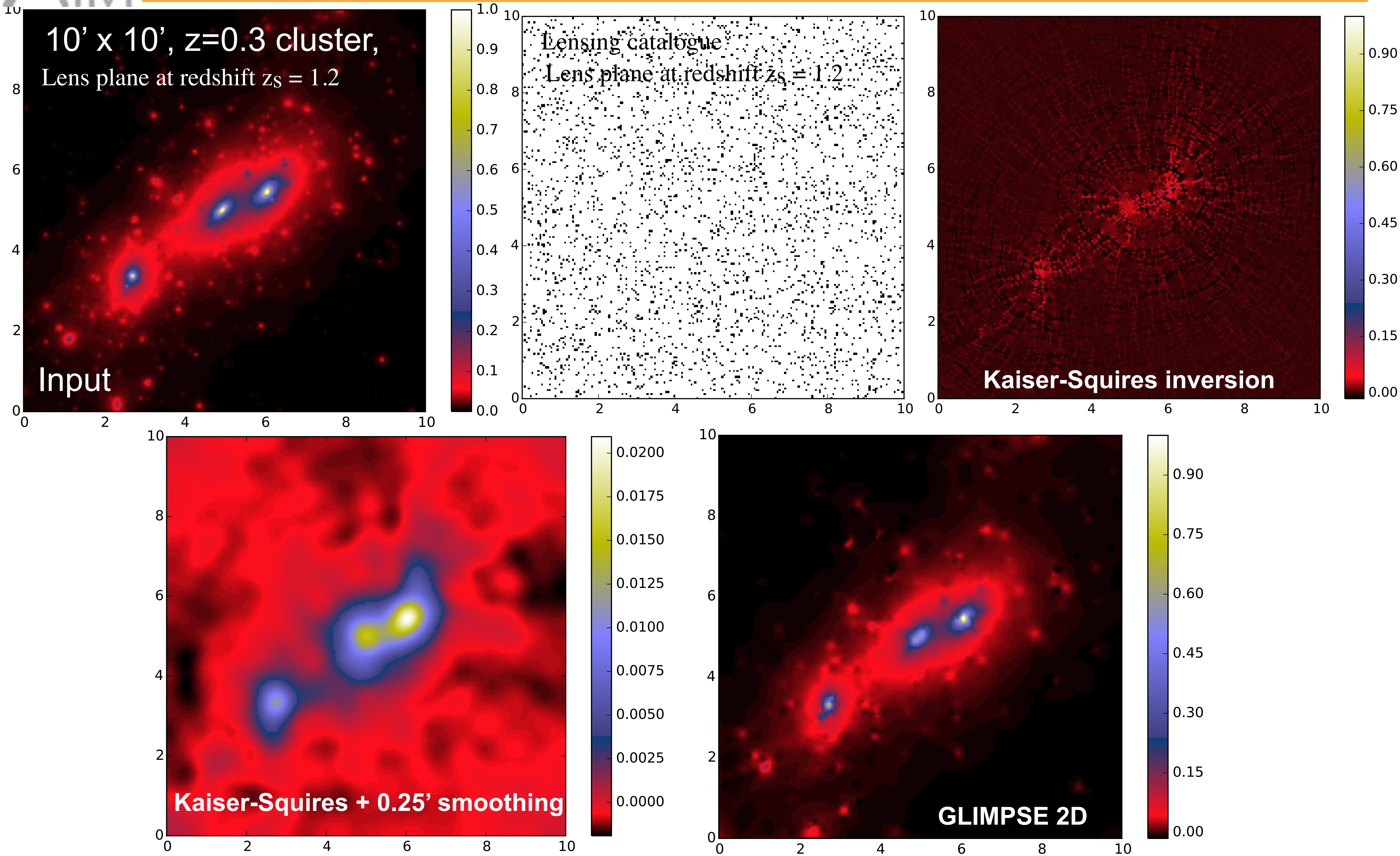


CosmoStat Lab

**Galaxy distribution:** **93% of missing pixels**, corresponding to 30 galaxies per square arcminute

# Missing Data + Noise

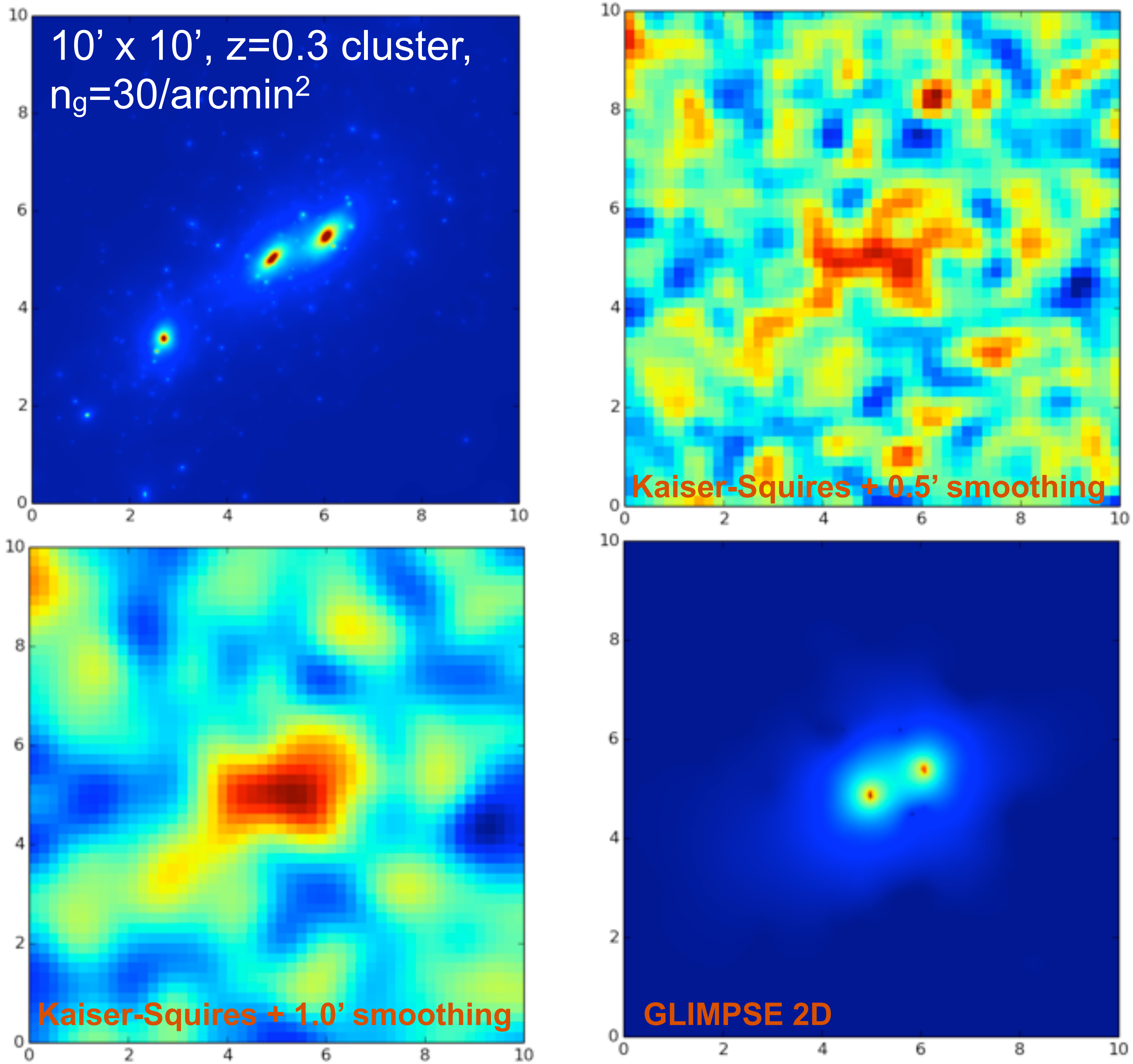

# A520

M.J. JEE , H.. HOEKSTRA , A. MAHDAVI , AND A. BABUL, HUBBLE SPACE TELESCOPE/ADVANCED CAMERA FOR SURVEYS CONFIRMATION OF THE DARK SUBSTRUCTURE IN A5201, Astrophysical Journal, Volume 783, Issue 2, article id. 78, 18 pp. (2014).

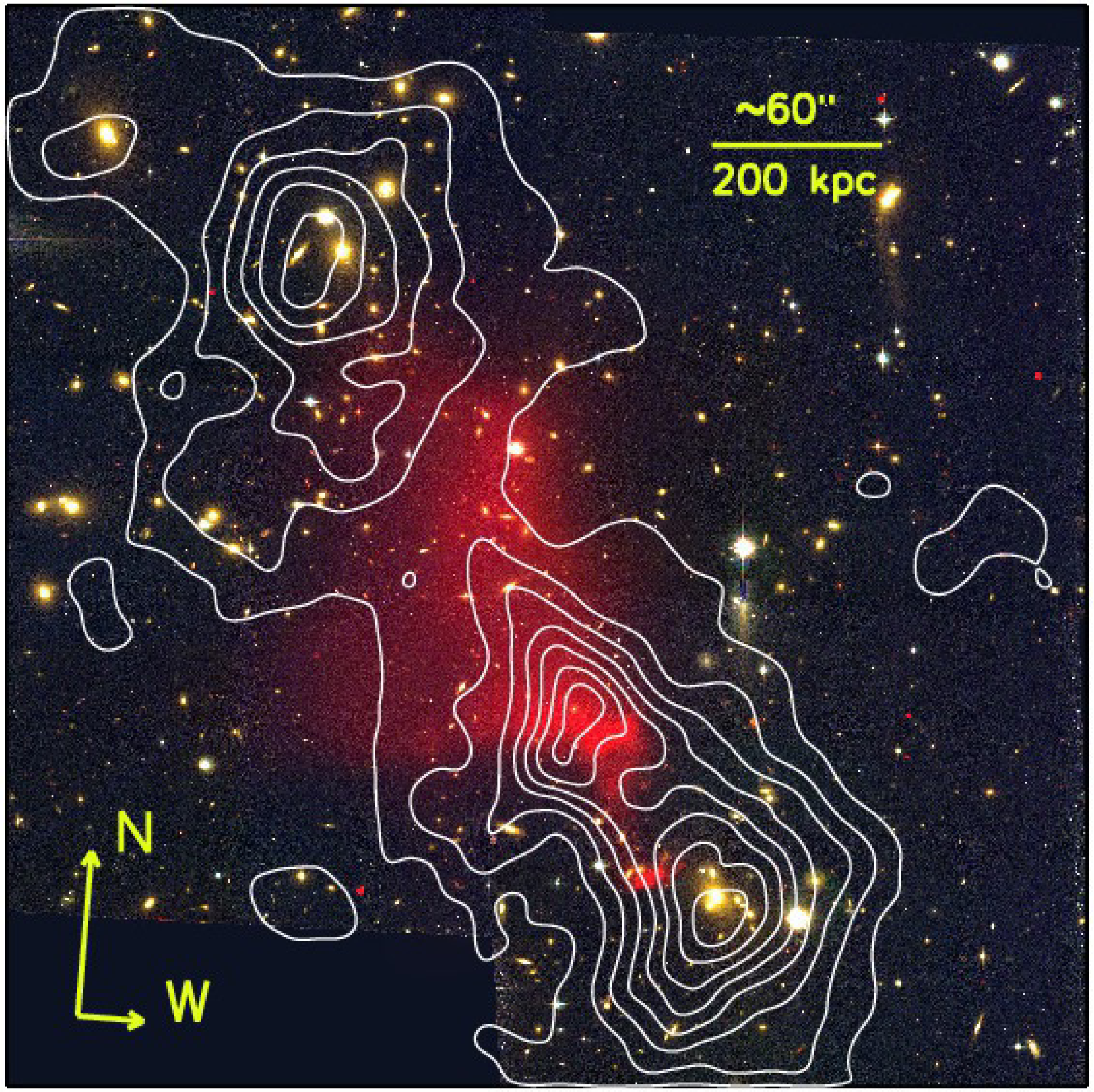


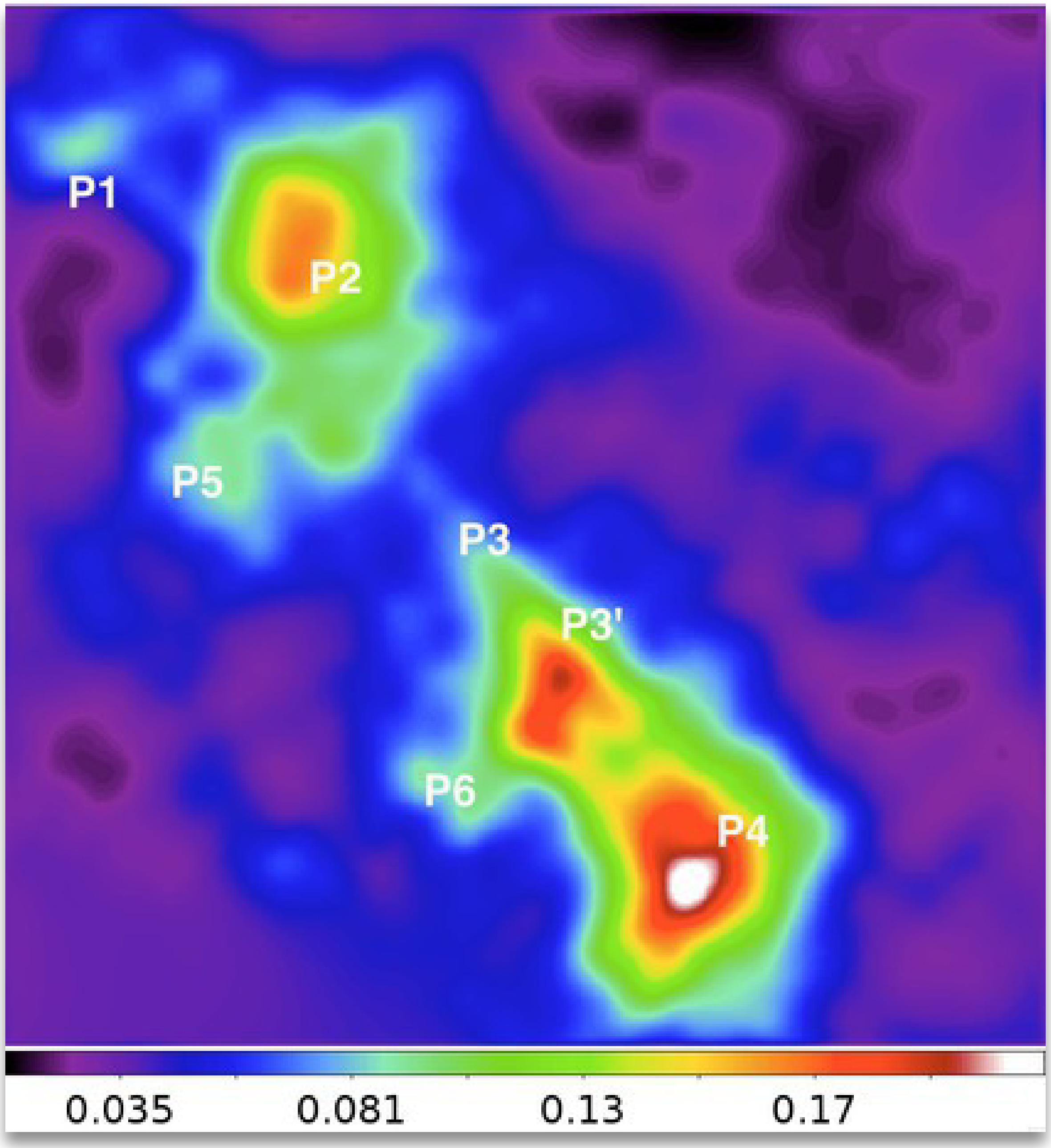

# Very preliminary results

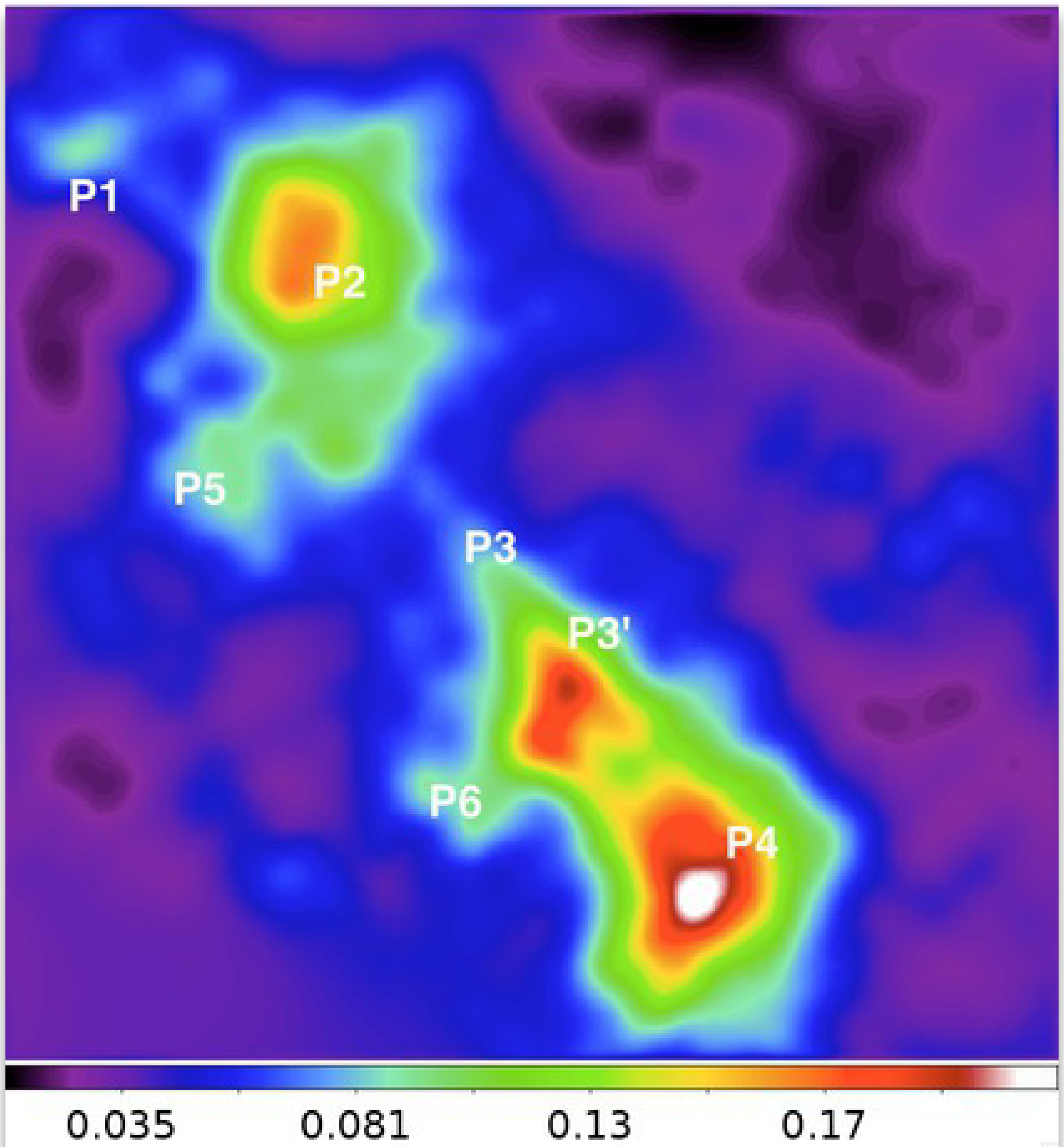


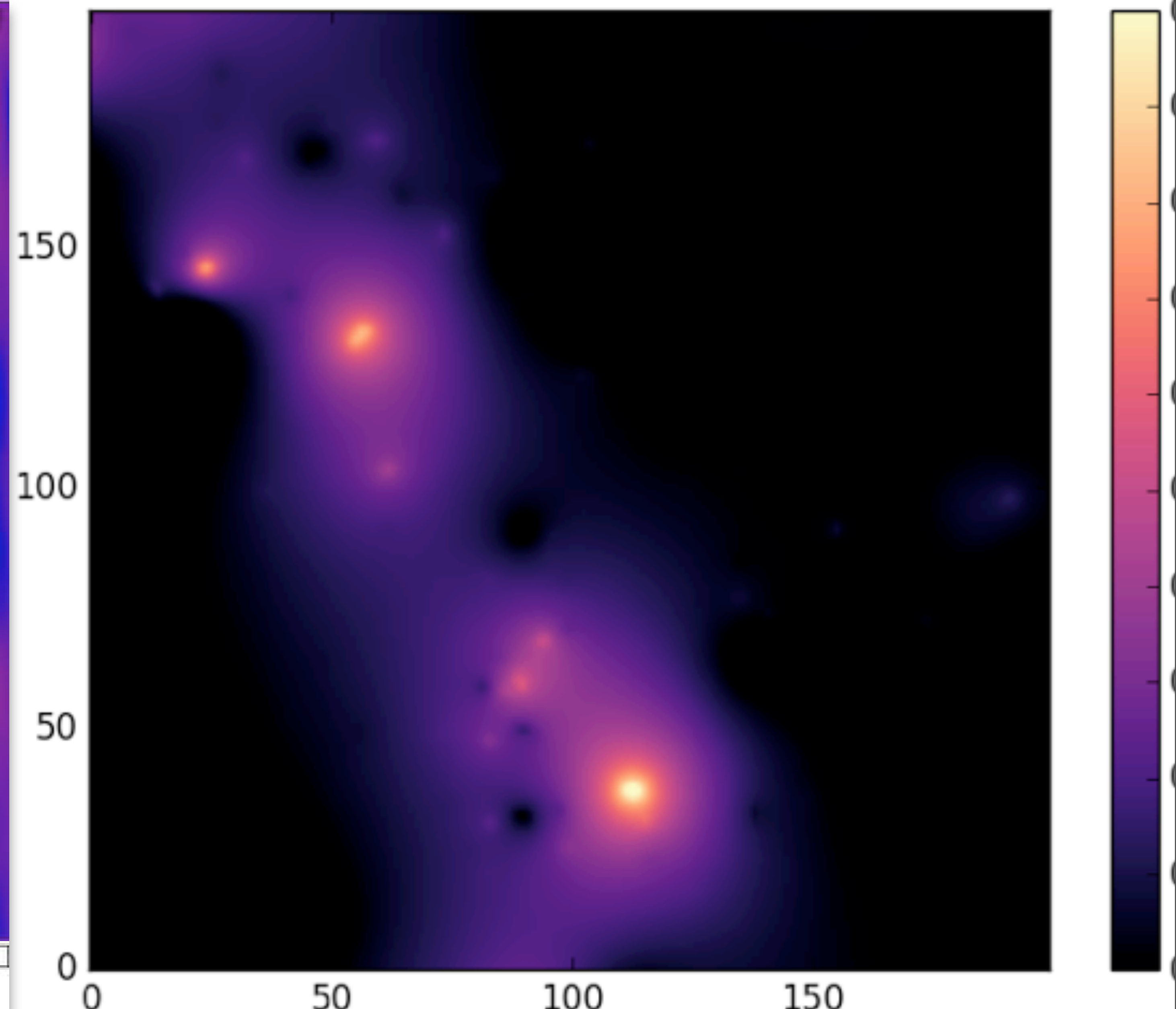

# Very preliminary results

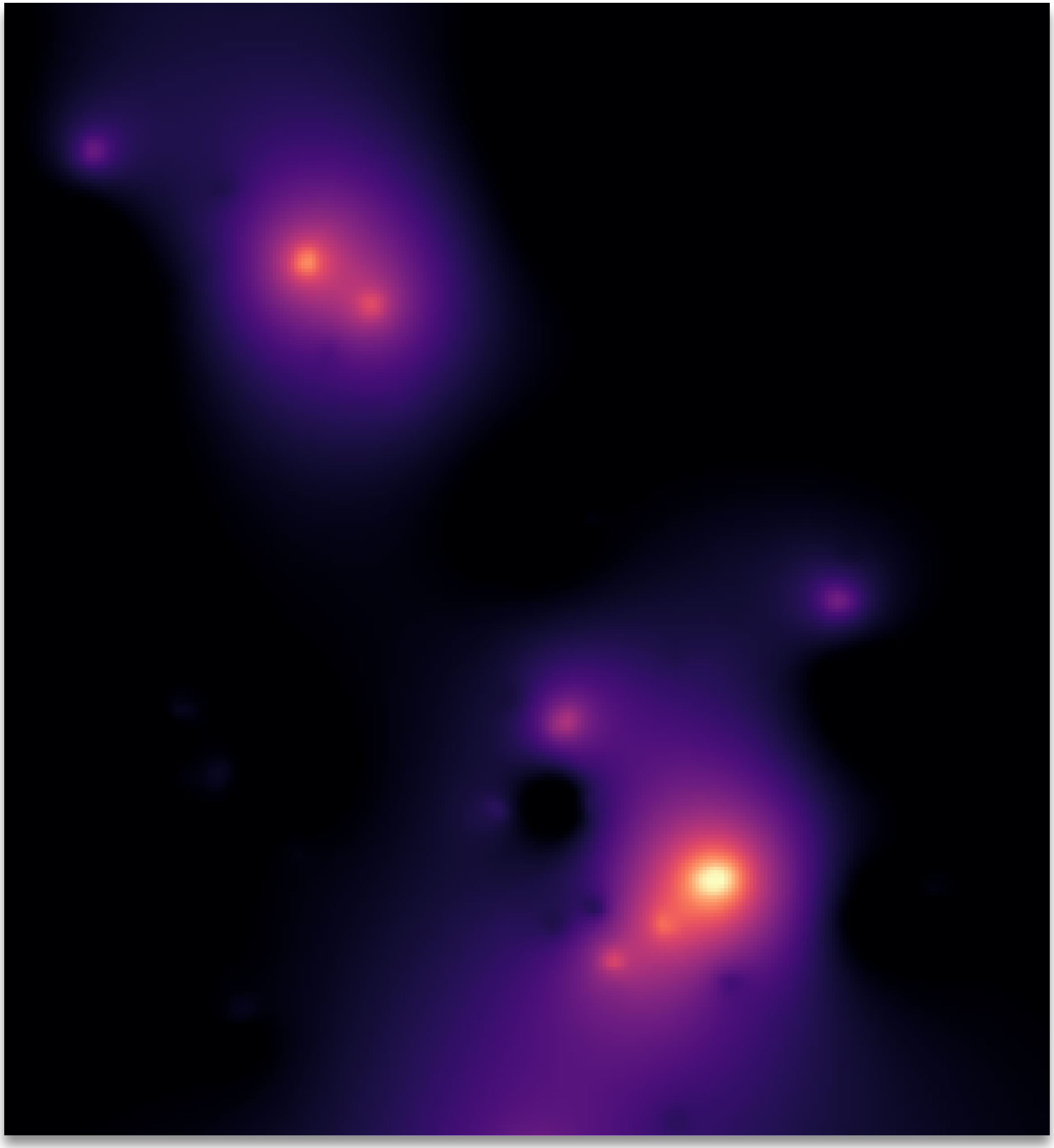

3 sigma using weights

# Very preliminary results

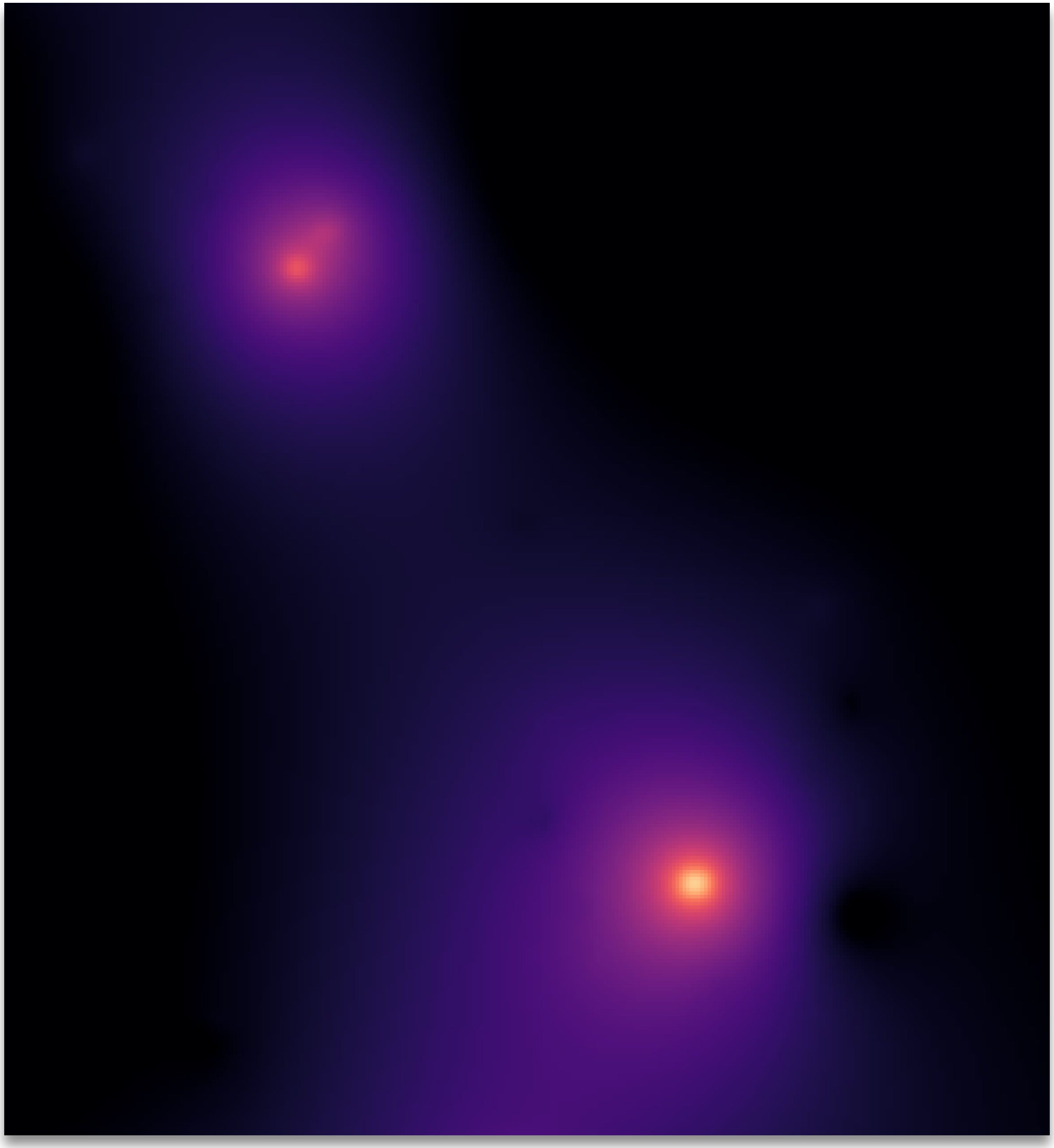

4 sigma using weights

CosmoStat Lab

# 3D Mass Mapping

$$\gamma(\boldsymbol{\theta}) = \frac{1}{\pi} \int d^2\boldsymbol{\theta}' \mathcal{D}(\boldsymbol{\theta} - \boldsymbol{\theta}')\kappa(\boldsymbol{\theta}')$$

Kappa (or convergence) is a dimensionless surface mass density of the lens

$$\kappa(\boldsymbol{\theta}, w) = \frac{3H_0^2\Omega_M}{2c^2} \int_0^w dw' \frac{f_K(w')f_K(w-w')}{f_K(w)} \frac{\delta[f_K(w')\boldsymbol{\theta}, w']}{a(w')},$$

$f_K$ is the angular diameter distance, which is a function of the comoving radial distance r and the curvature K.

$$\boldsymbol{\gamma} = \mathbf{P}_{\gamma\kappa}\boldsymbol{\kappa} + \boldsymbol{n}_\gamma,$$

$$\kappa = Q\delta + n$$

$$\boxed{\gamma = \mathbf{R}\delta + n}$$

- Galaxies are not intrinsically circular: intrinsic ellipticity ~ 0.2-0.3; gravitational shear ~ 0.02
- Reconstructions require knowledge of distances to galaxies

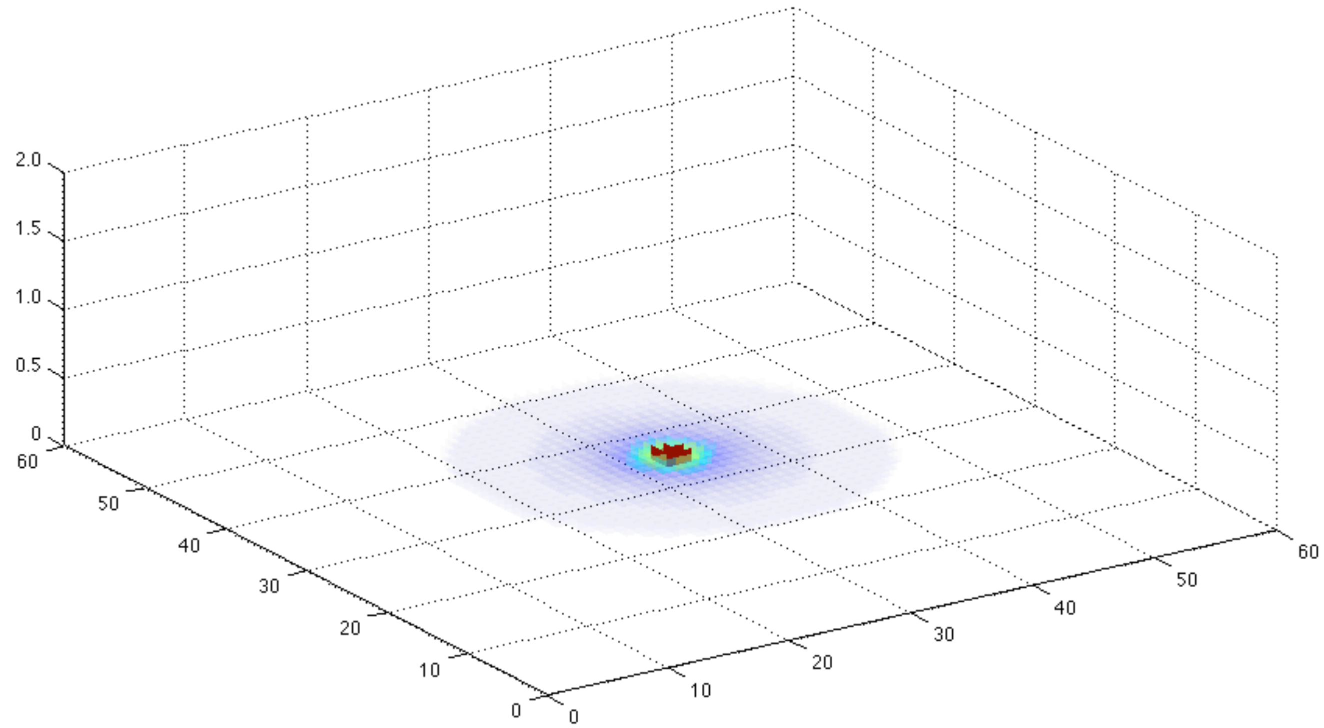
2.0
1.5
1.0
0.5
0
60
50
40
30
20
10
0
0
10
20
30
40
50
60

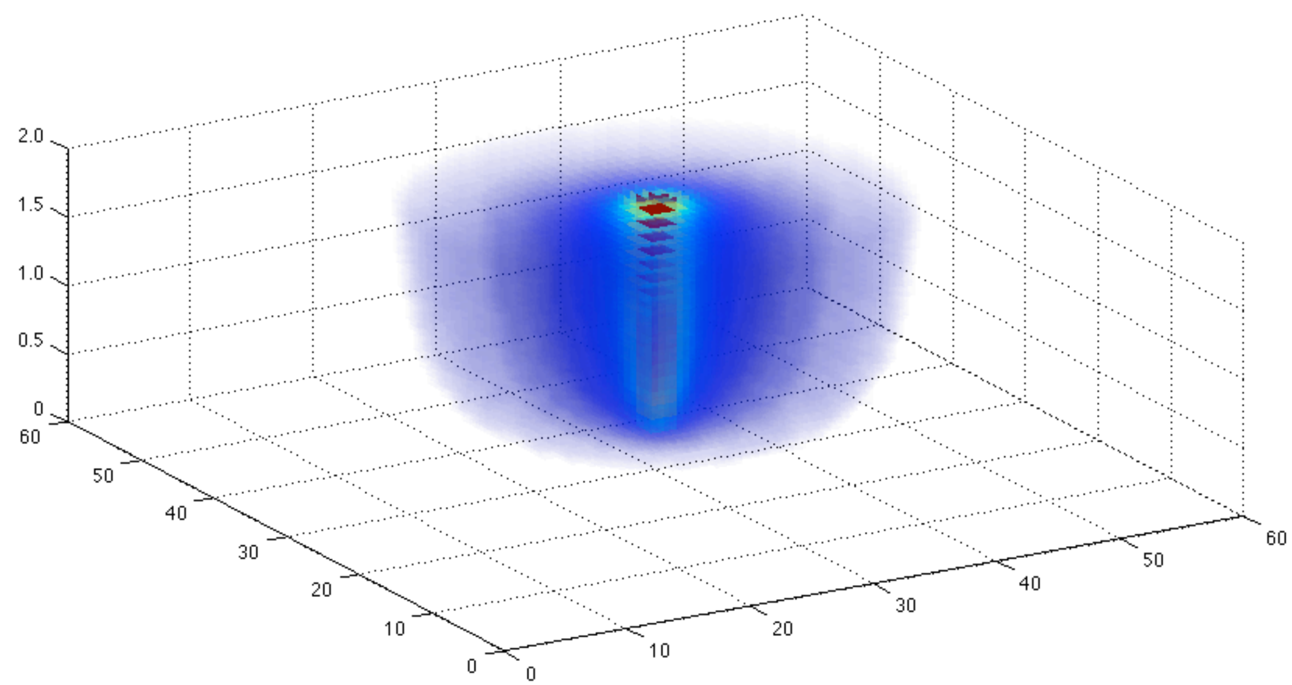
2.0
1.5
1.0
0.5
0
60
50
40
30
20
10
0
0
10
20
30
40
50
60

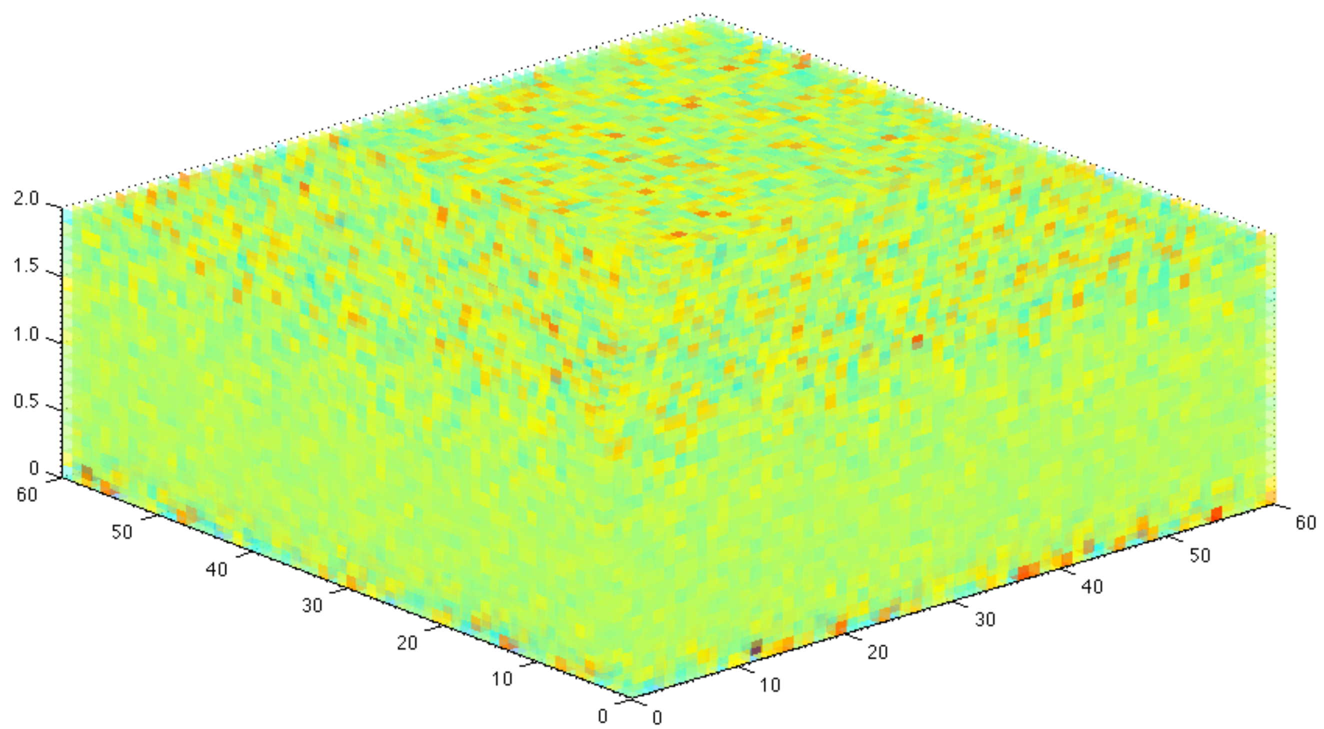
2.0
1.5
1.0
0.5
0
60
50
40
30
20
10
0
0
10
20
30
40
50
60

# Linear Methods

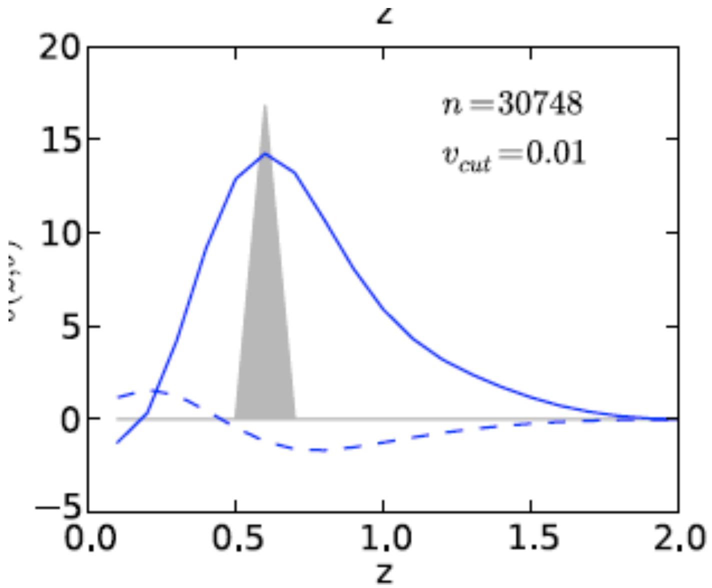


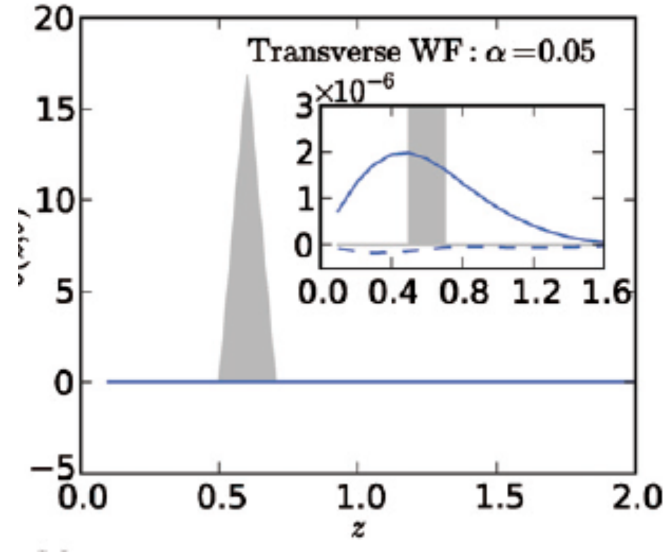


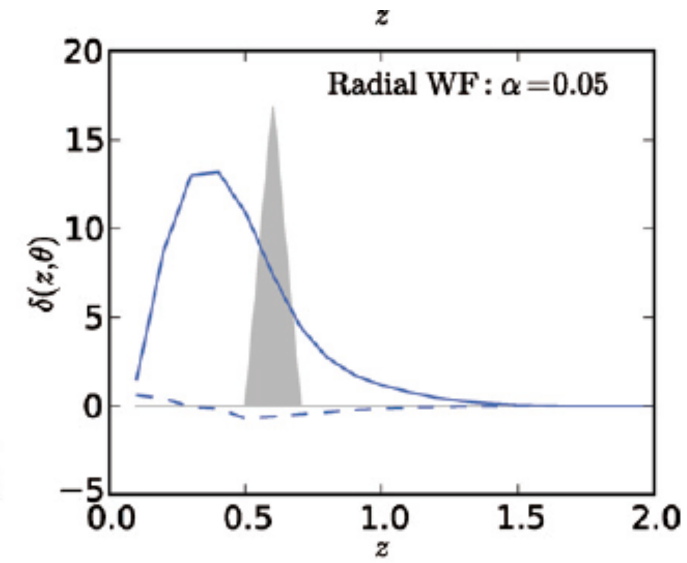


**Sparsity Recovery leads to Strong Improvement on**

- ✧ **Redshift bias** in location of detected peaks
- ✧ **Smearing** along the line of sight
- ✧ **Damping** of the reconstruction
- ✧ **Sensitivity** at high redshift
- ✧ Improving **resolution** in reconstructions

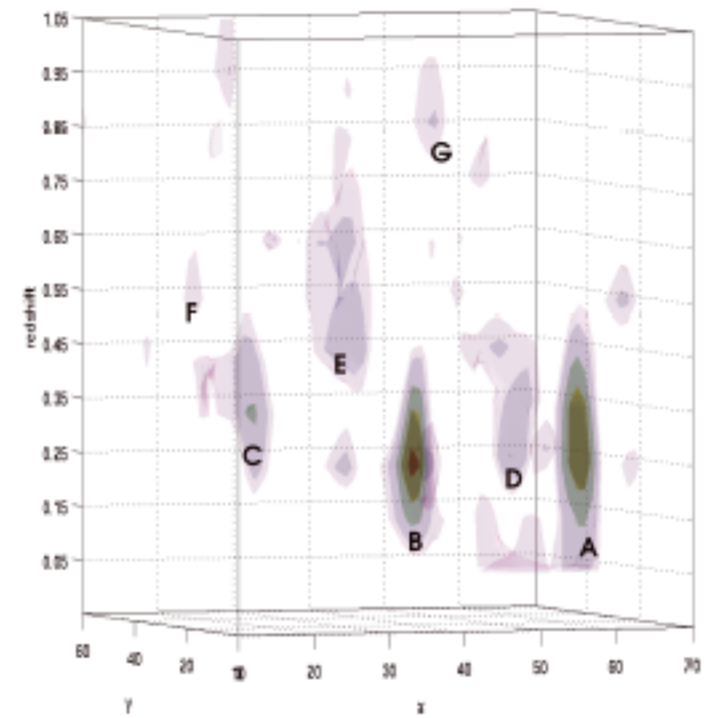

# Weak Lensing & 3D Matter Distribution

A. Leonard, F.X. Dupe, and J.-L. Starck, "A Compressed Sensing Approach to 3D Weak Lensing", **Astronomy and Astrophysics**, 539, A85, 2012.

A. Leonard, F. Lanusse, J-L. Starck, GLIMPSE: Accurate 3D weak lensing reconstruction usiing sparsity, Astronomy and Astrophysics, A&A, 2014.

$$\gamma = P\kappa \qquad \kappa = Q\delta$$

$$\delta = \Phi\alpha \quad \longrightarrow \quad \gamma = PQ\Phi\alpha = R\Phi\alpha$$

$$R = PQ \qquad \alpha$$

$\gamma$

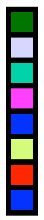

$=$

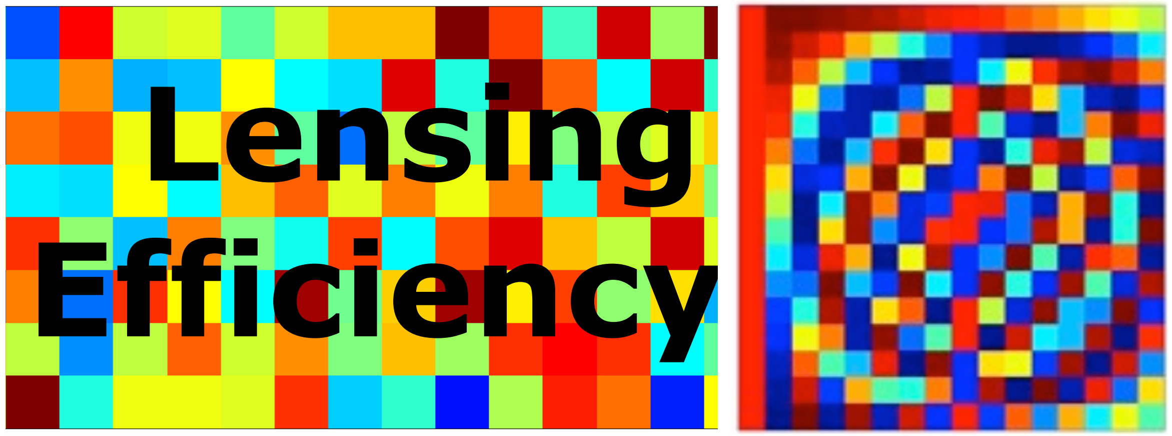


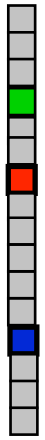

**Shear Measurements**
M measurements: number of bins in the source plan x number of pixels at for given bin

**Density constrast wavelet coefficients**

**==> Use Sparse recovery and Proximal optimization theory**

$$\min_{\delta} \frac{1}{2} \parallel \gamma - R\delta \parallel^2_{\Sigma^{-1}} + \lambda \parallel \Phi^t \delta \parallel_1$$

$\delta = \Phi\alpha$ $\qquad \Phi$ = 2D Wavelet Transform on each redshift bin

# WL 3D Cosmo-Door is now open

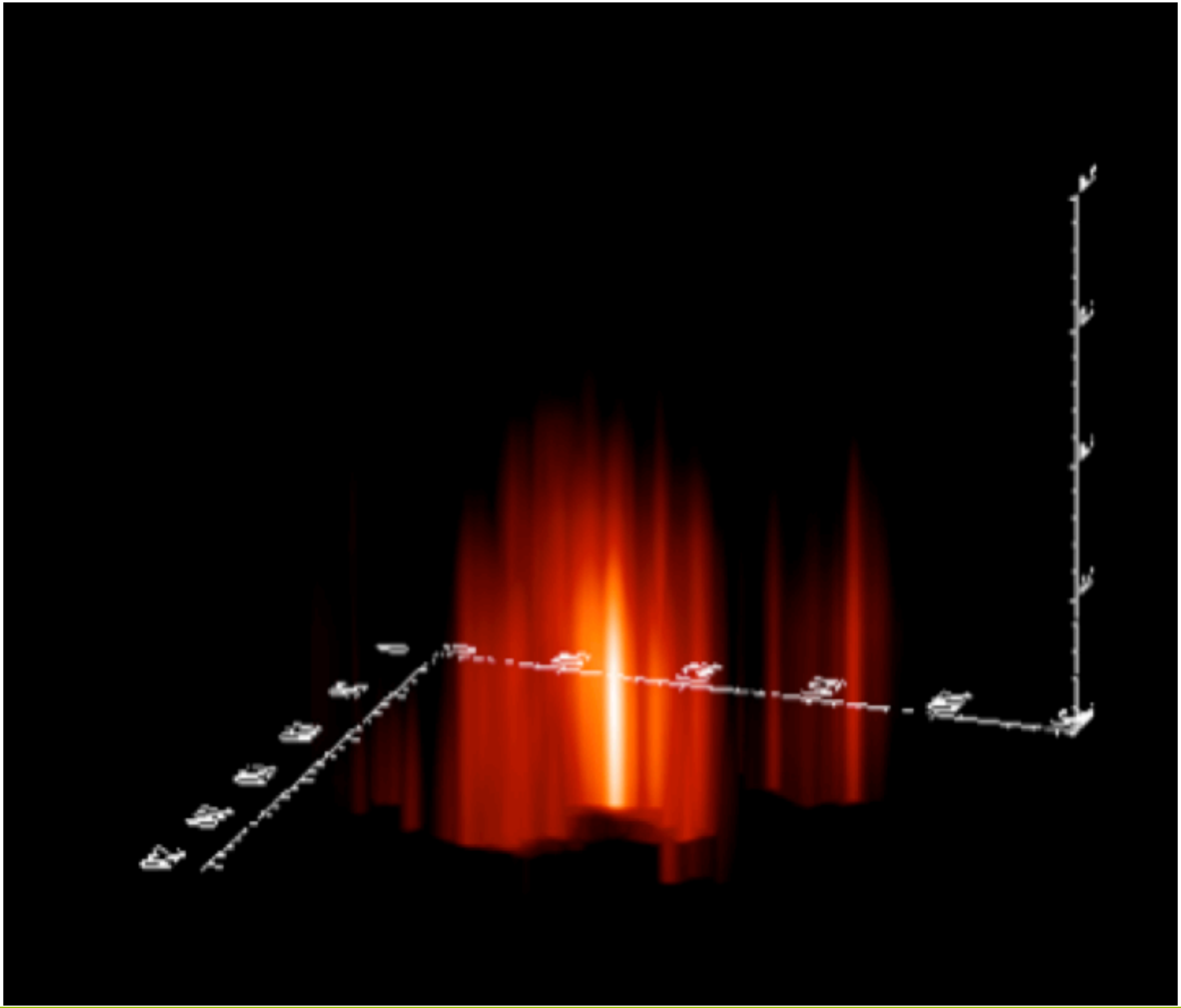

CosmoStat Lab

# Mass Estimation

## Cluster Masses from 3D Weak Lensing Reconstructions

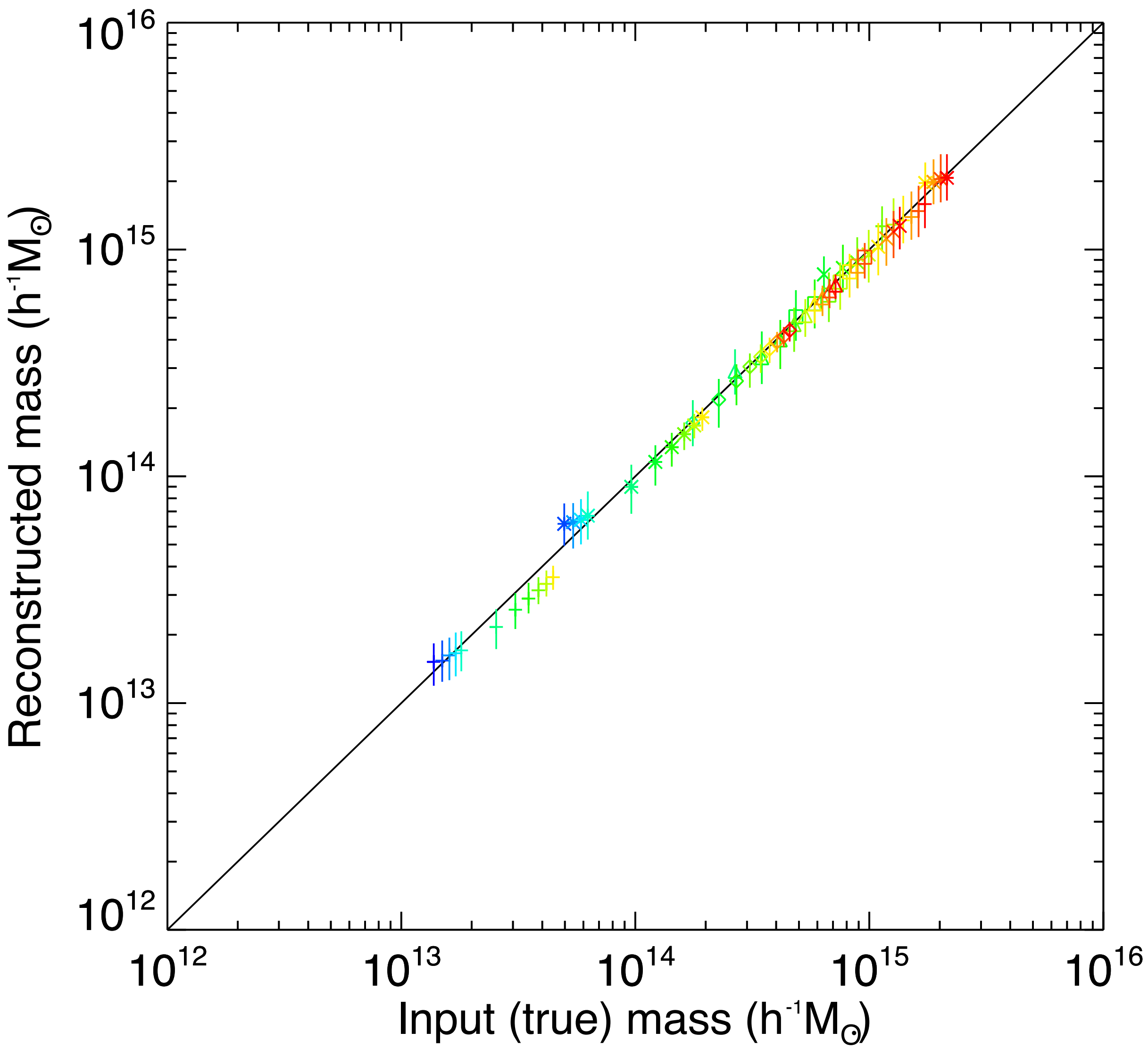


- GLIMPSE 3D reconstructions provide a direct, unbiased & nonparametric estimate of the cluster mass (Leonard, Lanusse & Starck 2014, MNRAS, 440, 1281)
- Masses estimated integrating the density in the central 4 x 4 arcmin
- Error bars reflect the standard deviation in mass estimates 1000 Monte Carlo simulations of each cluster
- Cluster masses $2 \times 10^{13} h^{-1} M_\odot \leq M_{vir} \leq 10^{15} h^{-1} M_\odot$
- Cluster redshifts $0.05 \leq z \leq 0.75$

A. Leonard, F. Lanusse, & J.-L. Starck 2015, MNRAS

# Cluster Detections: 2D vs 3D mapping

- 3D reconstructions (GLIMPSE) may offer an SNR advantage over 2D reconstructions (MRLens) for the detection of clusters.
- Improvement particularly significant at high redshift.

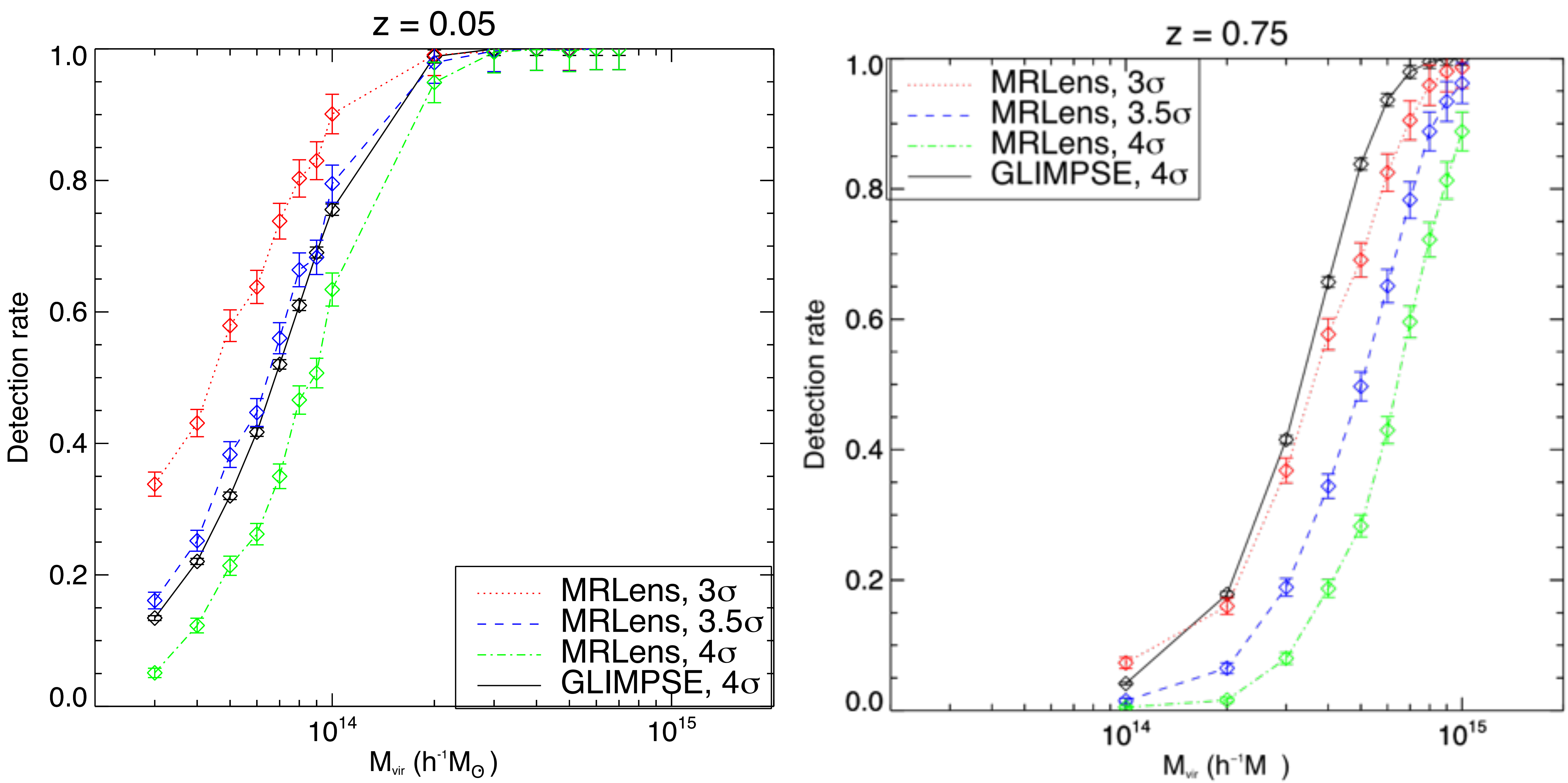


A. Leonard, F. Lanusse, & J.-L. Starck 2015, MNRAS

# Redshift Estimation: TMF vs GLIMPSE

Blue dots: GLIMPSE z estimates

- Colored dots: TMF z estimates for

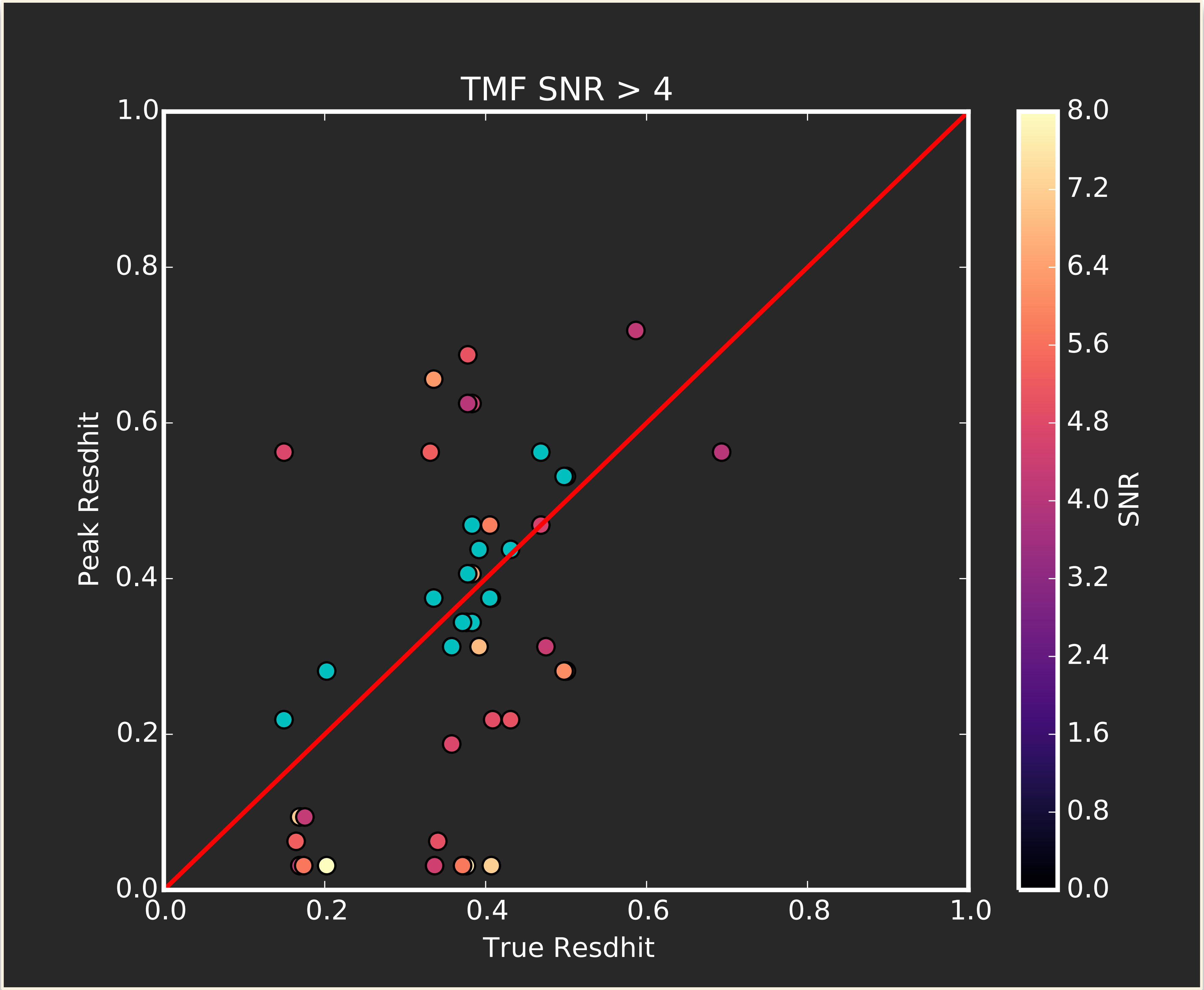


- GLIMPSE recovers more accurate z's

# Planck Component Separation

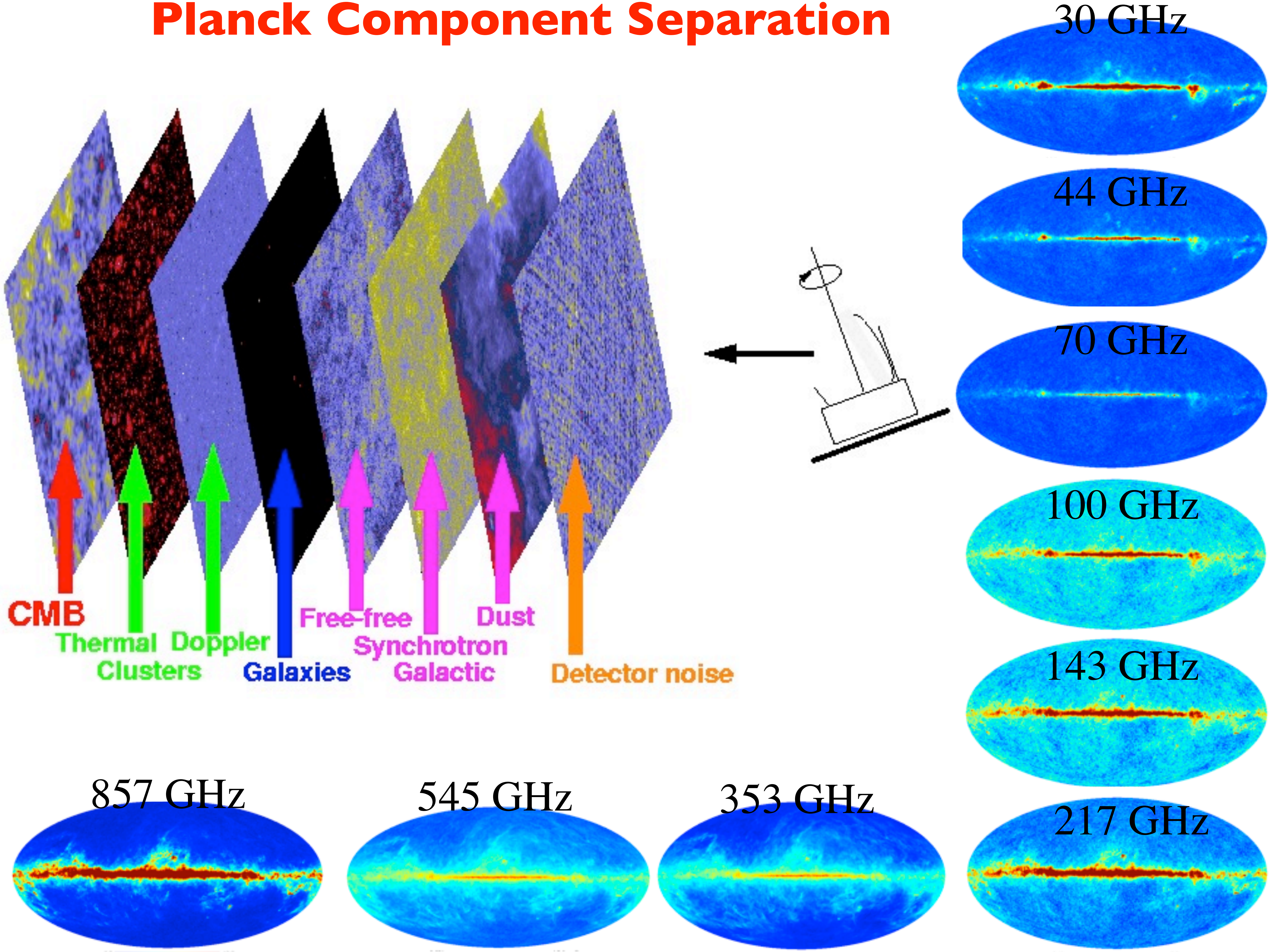

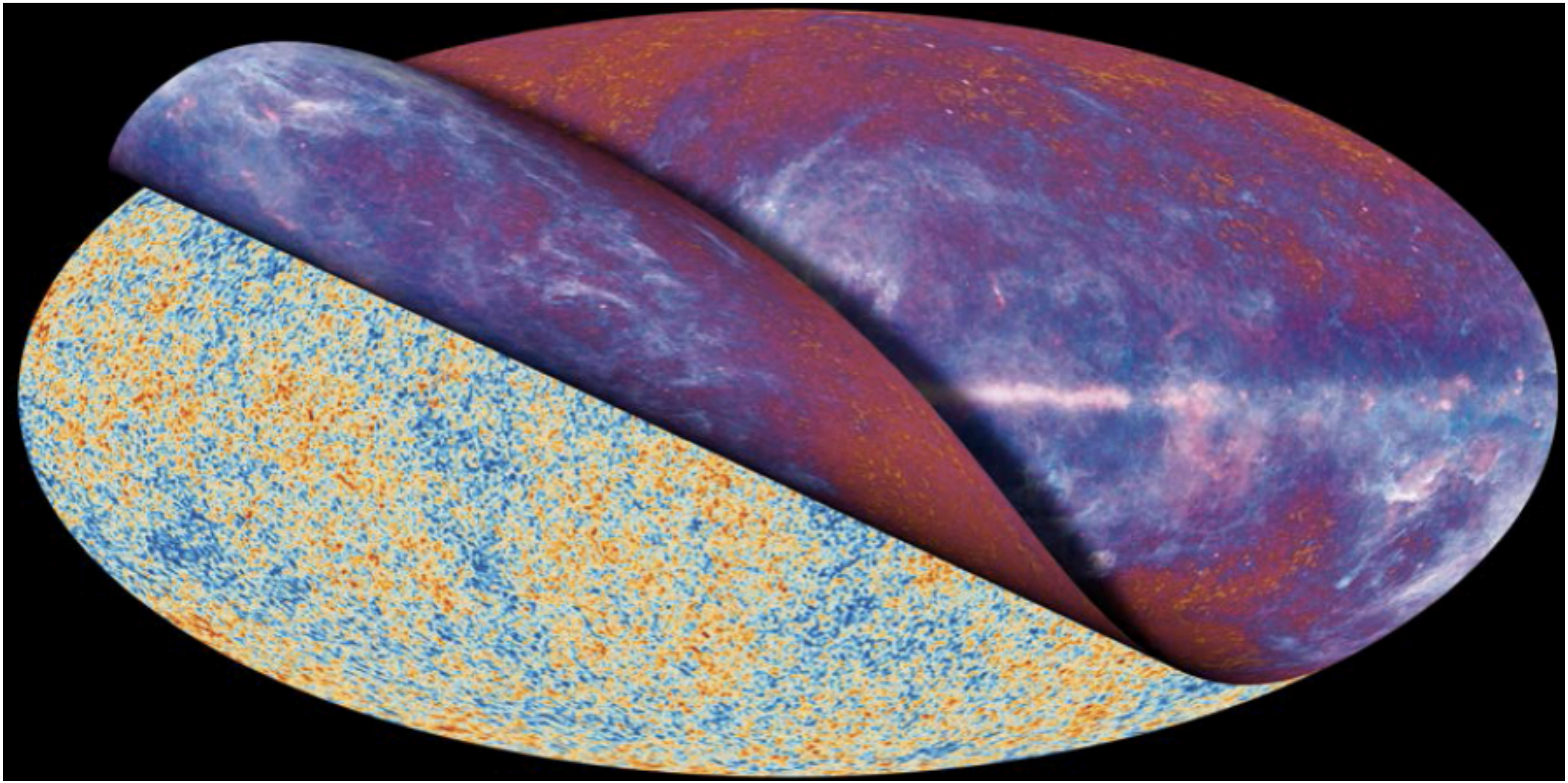

# Sparse Component Separation: the GMCA Method

**A and X are estimated alternately and iteratively in two steps :**

•J. Bobin, J.-L. Starck, M.J. Fadili, and Y. Moudden, "Sparsity, Morphological Diversity and Blind Source Separation", IEEE Trans. on Image Processing, Vol 16, No 11, pp 2662 - 2674, 2007.
•.J. Bobin, J.-L. Starck, M.J. Fadili, and Y. Moudden, "Blind Source Separation: The Sparsity Revolution", Advances in Imaging and Electron Physics , Vol 152, pp 221 -- 306, 2008.

$$\mathbf{Y} = \mathbf{A}\mathbf{X}$$

**1) Estimate X assuming A is fixed :**

$$\{X\} = \mathrm{Argmin}_X \|\mathbf{Y} - \mathbf{A}\mathbf{X}\|^2_{F,\mathbf{\Sigma}} + \sum_j \lambda_j \|\Phi^t x_j\|_1$$

=> Sparse coding (proximal theory, etc)

**2) Estimate A assuming X is fixed (a simple least square problem) :**

$$\{A\} = \mathrm{Argmin}_A \|\mathbf{Y} - \mathbf{A}\mathbf{X}\|^2_{F,\mathbf{\Sigma}}$$

=> Least square estimator

# Full Sky Sparse WMAP + Planck-PR2 Map

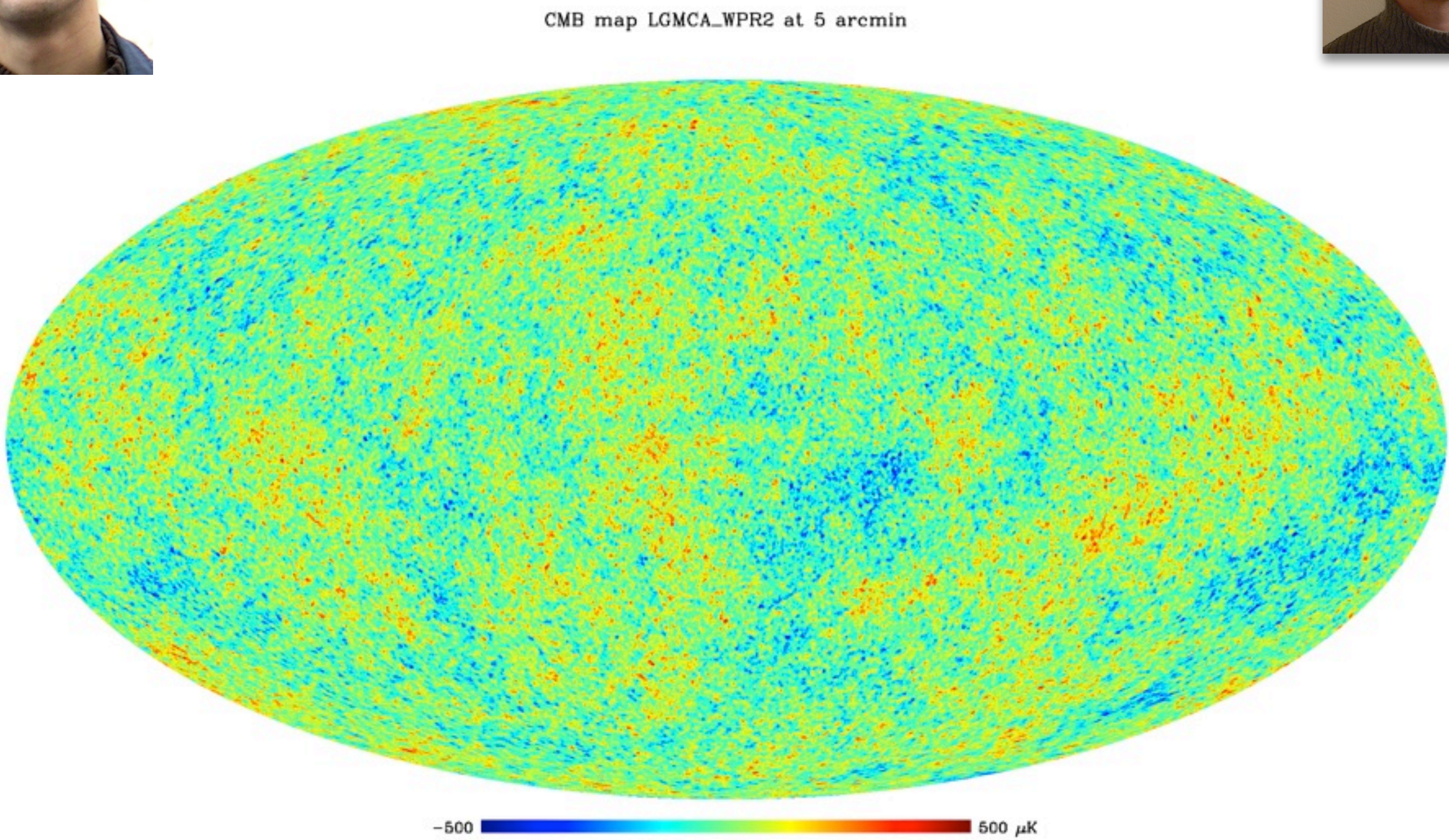


*Bobin J., Sureau F., Starck J-L, Rassat A. and Paykari P., Joint Planck and WMAP CMB map reconstruction, A&A, 563, 2014*

***Bobin J., Sureau F., Starck, CMB reconstruction from the WMAP and Planck PR2 data, submitted to A&A.***

# Traces of tSZ effect

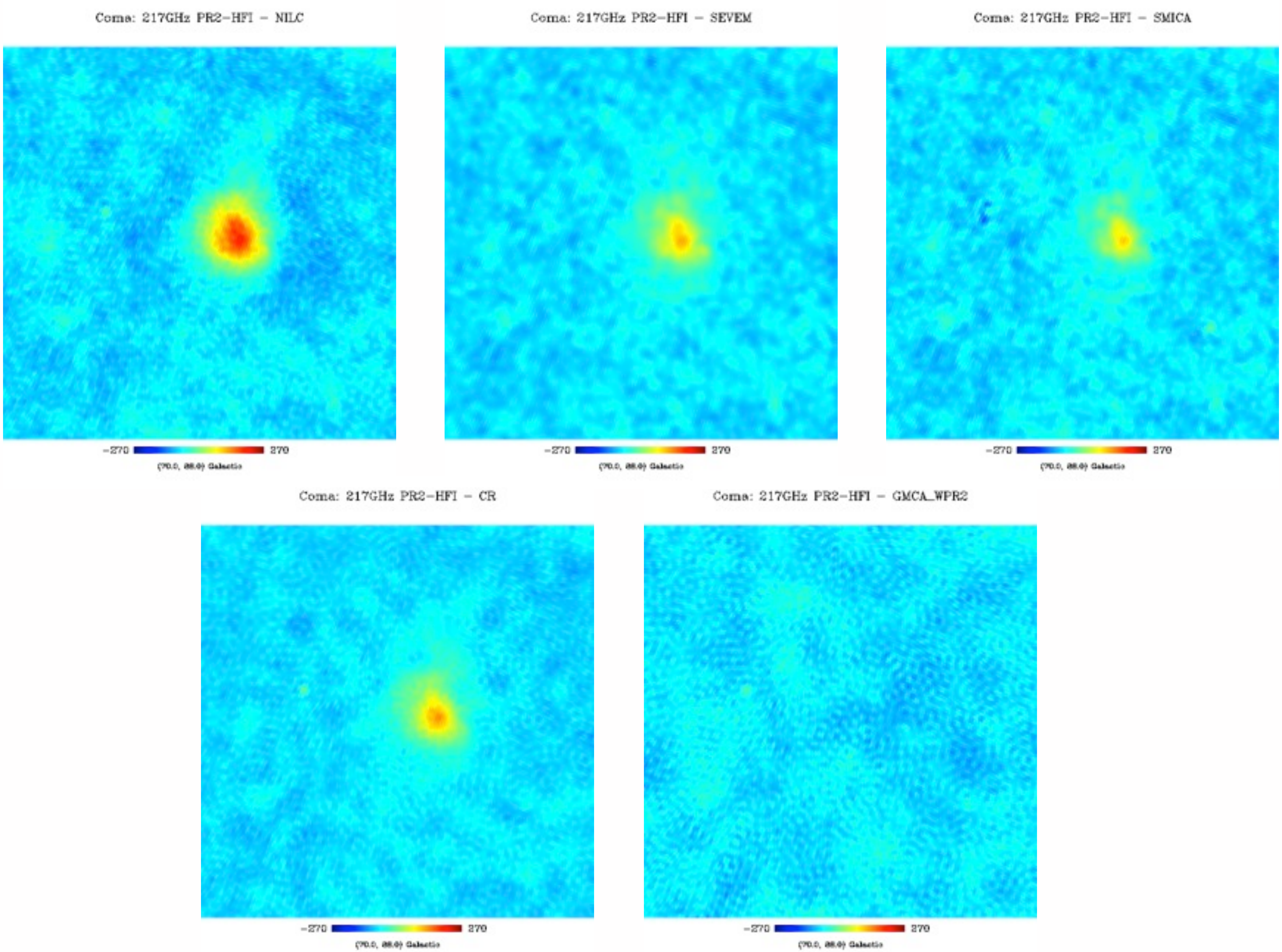

# Quality map

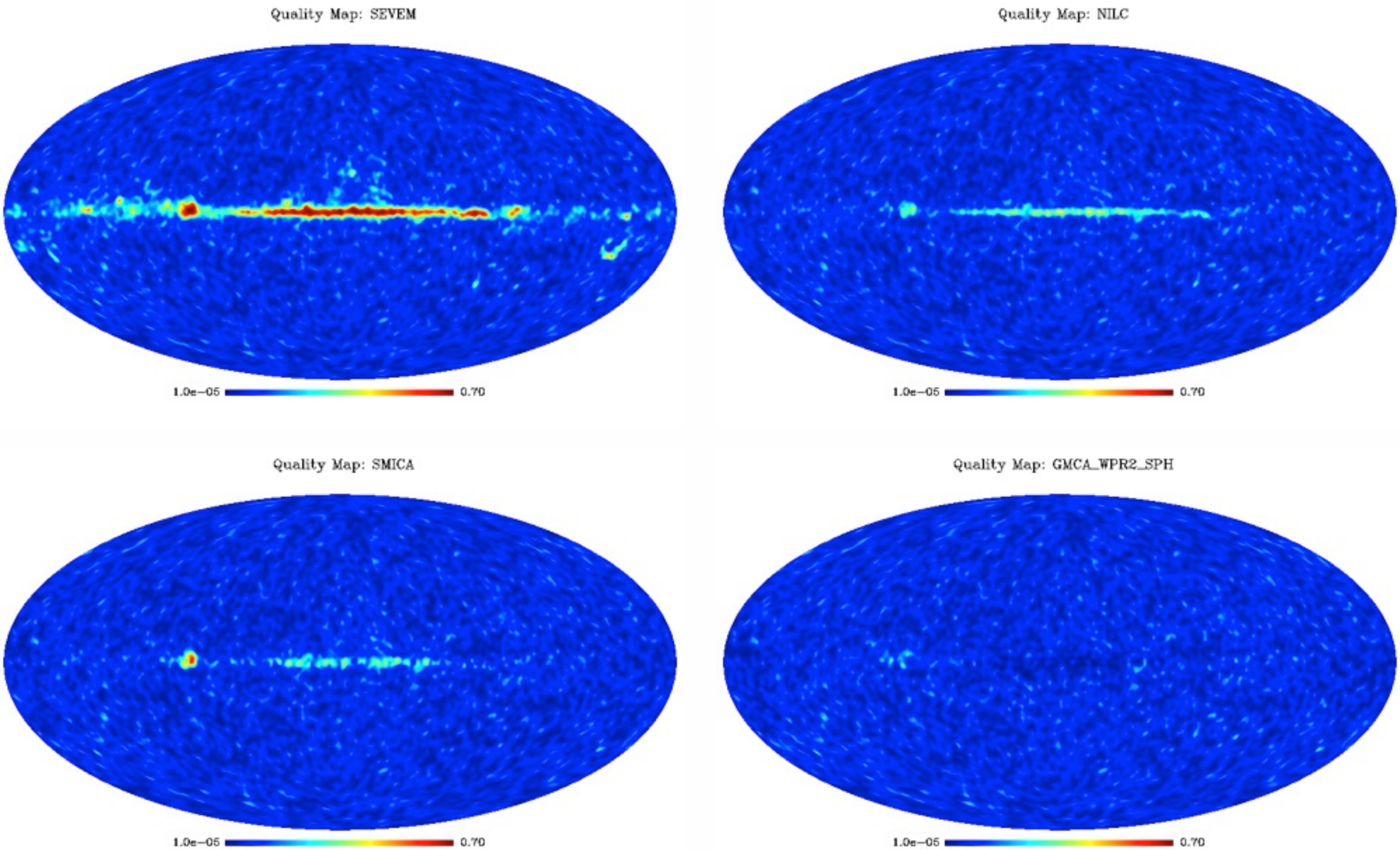
Quality Map: SEVEM
1.0e−05
0.70
Quality Map: NILC
1.0e−05
0.70
Quality Map: SMICA
1.0e−05
0.70
Quality Map: GMCA_WPR2_SPH
1.0e−05
0.70

# Radio interferometry & Compressed Sensing


$$H$$

$y$

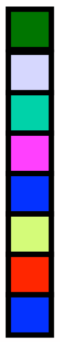

$=$

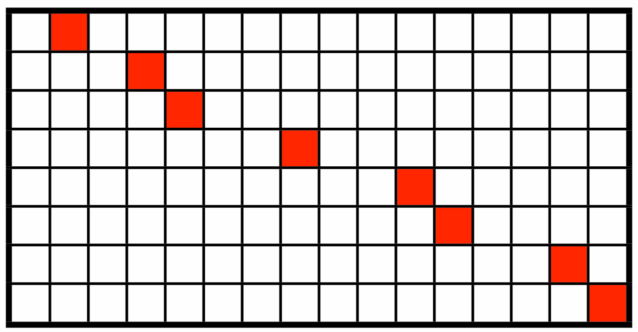

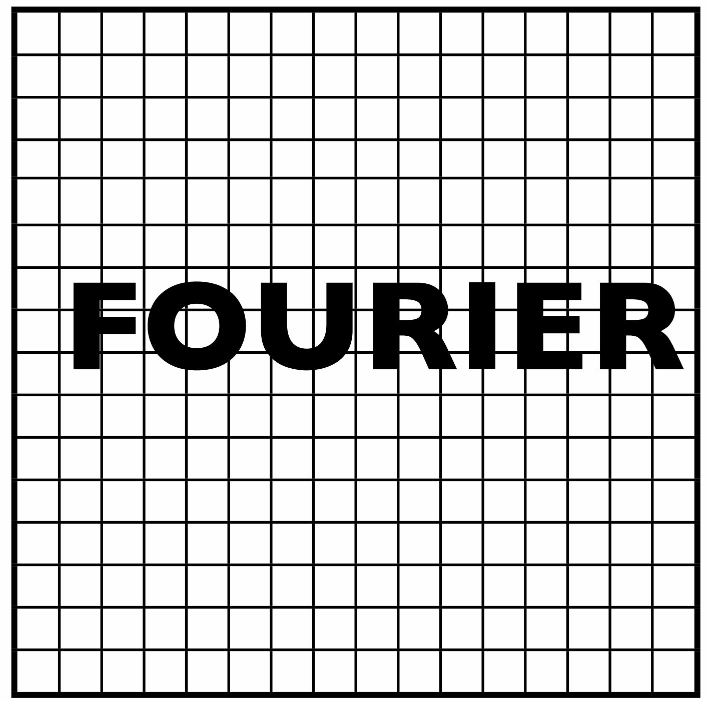


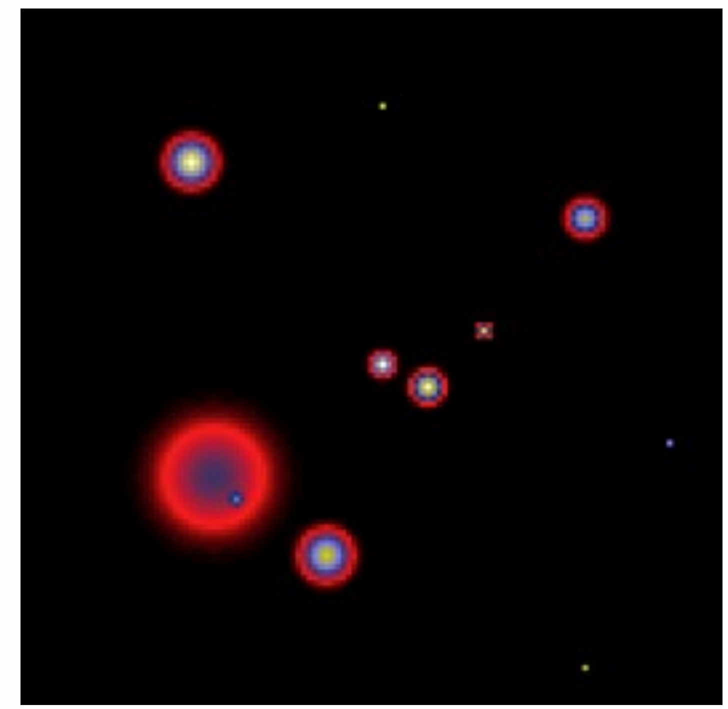

**Visibilities**

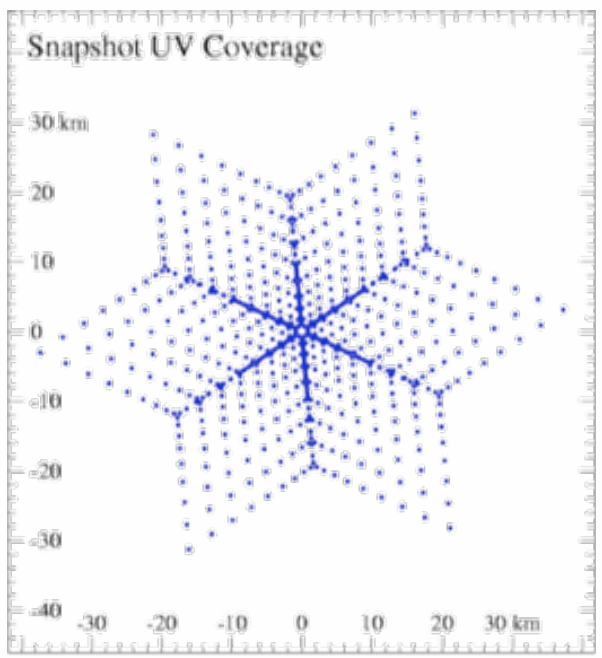


**Measurement matrix**
**(Fourier + Sampling)**

**Sky**

$X$

$$Y = HX + N$$

# Compressed Sensing & LOFAR Cygnus A Data

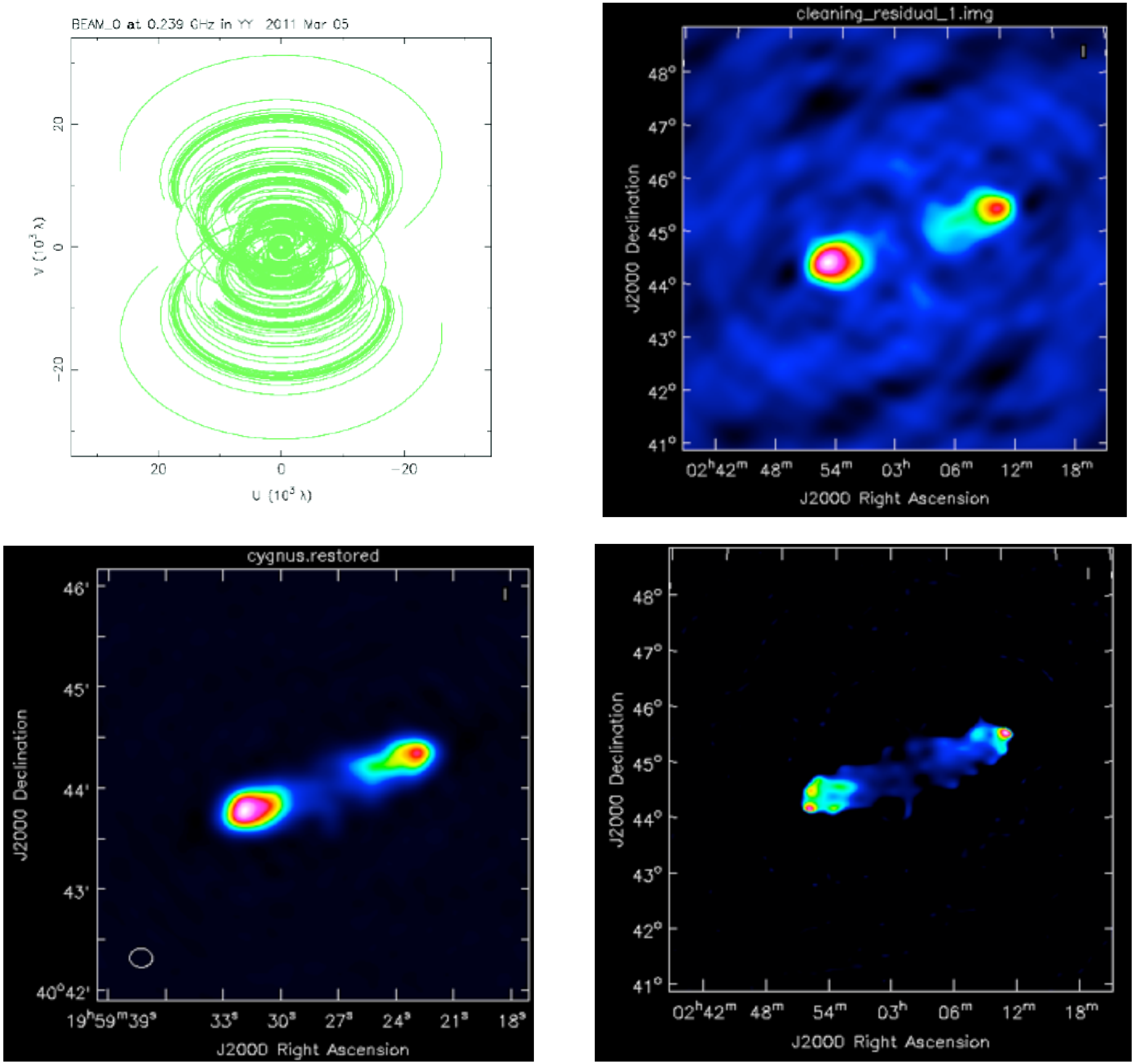


Garsden et al, "**LOFAR Image Sparse Reconstruction**", A&A, 575, A90, 2015.

http://arxiv.org/abs/1406.7242


J. Girard


H. Garsden


S. Corbel


C. Tasse

Garsden et al, “LOFAR Image Sparse Reconstruction”, A&A, 575, A90, 2015, ArXiv:1406.7242.

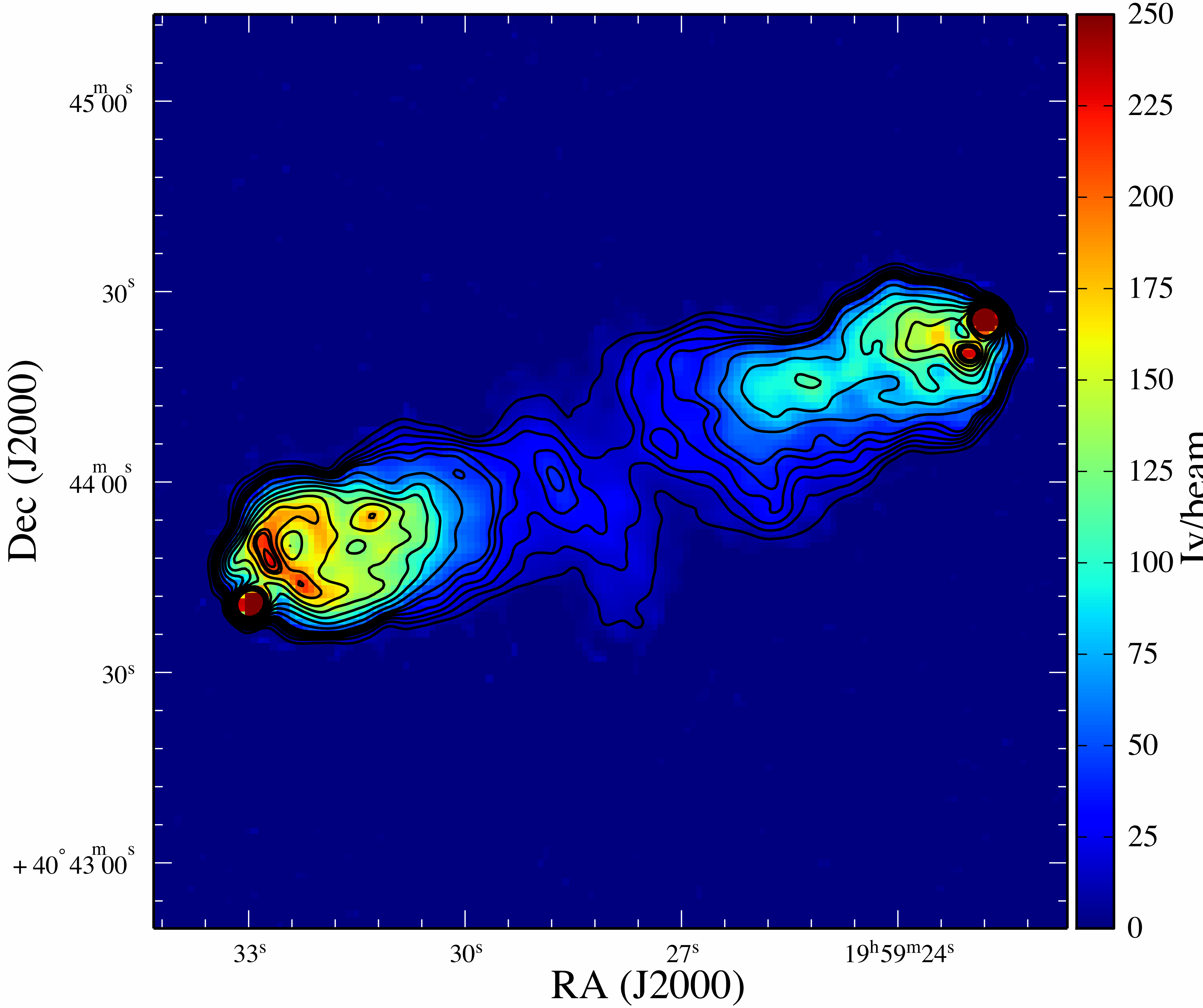


Colorscale: reconstructed 512x512 image of Cygnus A at 151 MHz (with resolution 2.8” and a pixel size of 1”). Contours levels are [1,2,3,4,5,6,9,13,17,21,25,30,35,37,40] Jy/Beam from a 327.5 MHz Cyg A VLA image (Project AK570) at 2.5” angular resolution and a pixel size of 0.5”. **Recovered features in the CS image correspond to real structures observed at higher frequencies.**

- **Exploit the information in time**


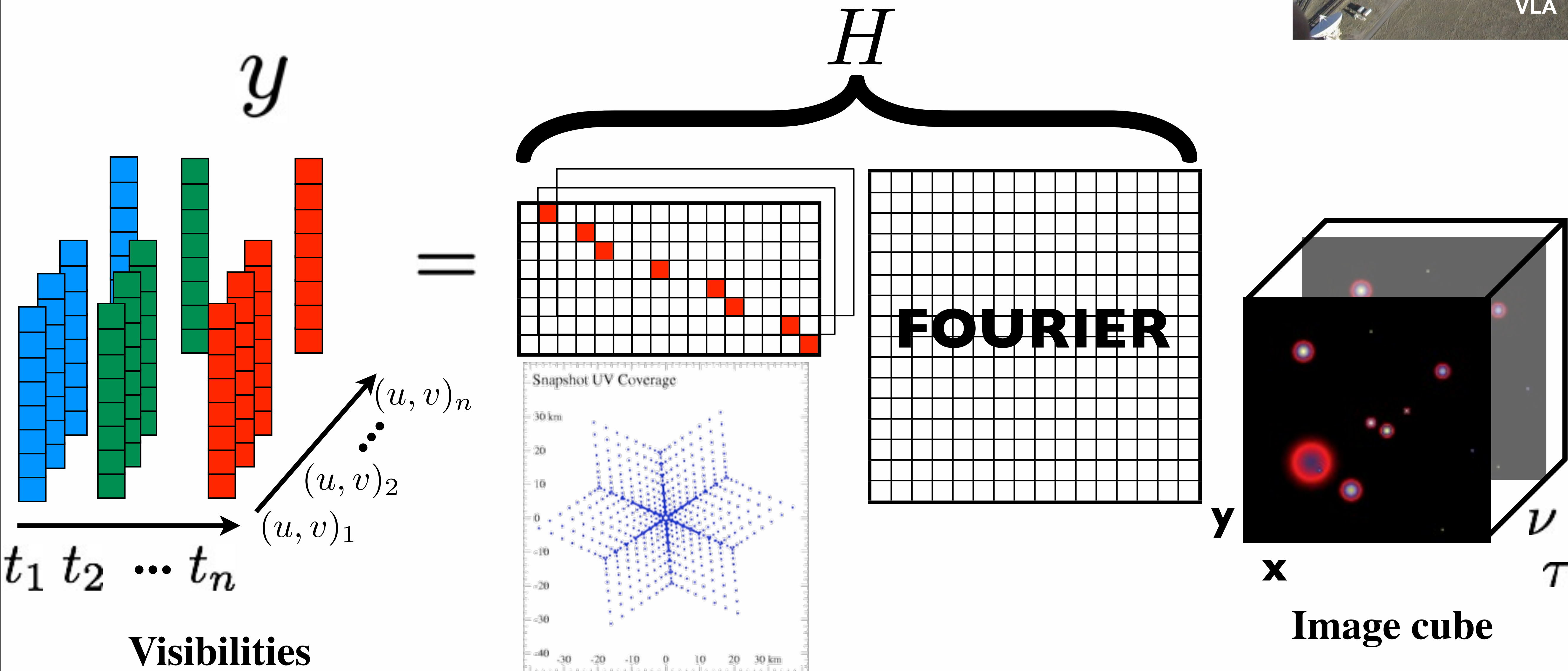


**Measurement matrix**
**(Fourier + Sampling)**

- **The masking operator will also be time-dependent**

# Ingredients 1/2

We need **dictionaries** - space and time are independent

$$\psi(x,y,t) = \psi^{(xy)}(x,y)\psi^{(t)}(t)$$

- **for the 2D spatial signal**

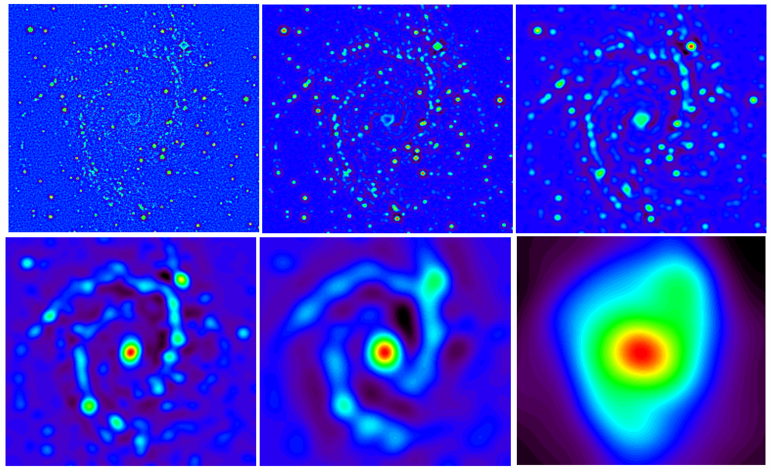

Starlets [Starck et al. 2011]

(Isotropic Undecimated Wavelet Transform)

$$\varphi = B_3 - \text{spline}, \quad \frac{1}{2}\psi(\frac{x}{2}) = \frac{1}{2}\varphi(\frac{x}{2}) - \varphi(x)$$

$$h = [1,4,6,4,1]/16, \quad g = \delta - h, \quad \tilde{h} = \tilde{g} = \delta$$

$$I(k,l) = c_{J,k,l} + \sum_{j=1}^{J} w_{j,k,l}$$

- **for the 1D temporal signal**

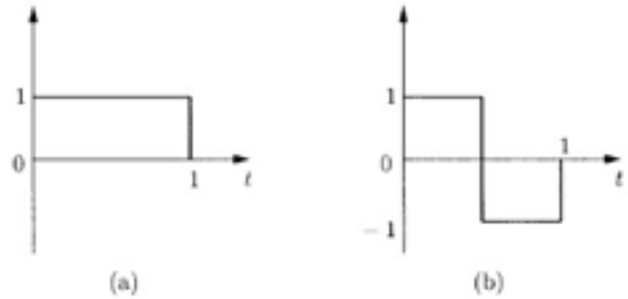


**Haar wavelets** Quantified signals

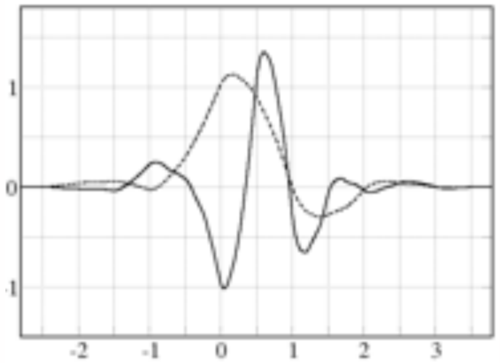


**7/9 wavelets** Semi-continuous

...

# 2D-1D Wavelet Decomposition

$$w_{j_1,j_2}[k_x,k_y,k_z] = D * \bar{\psi}^{(xy)}_{j_1} * \bar{\psi}^{(z)}_{j_2}(x,y,z)$$

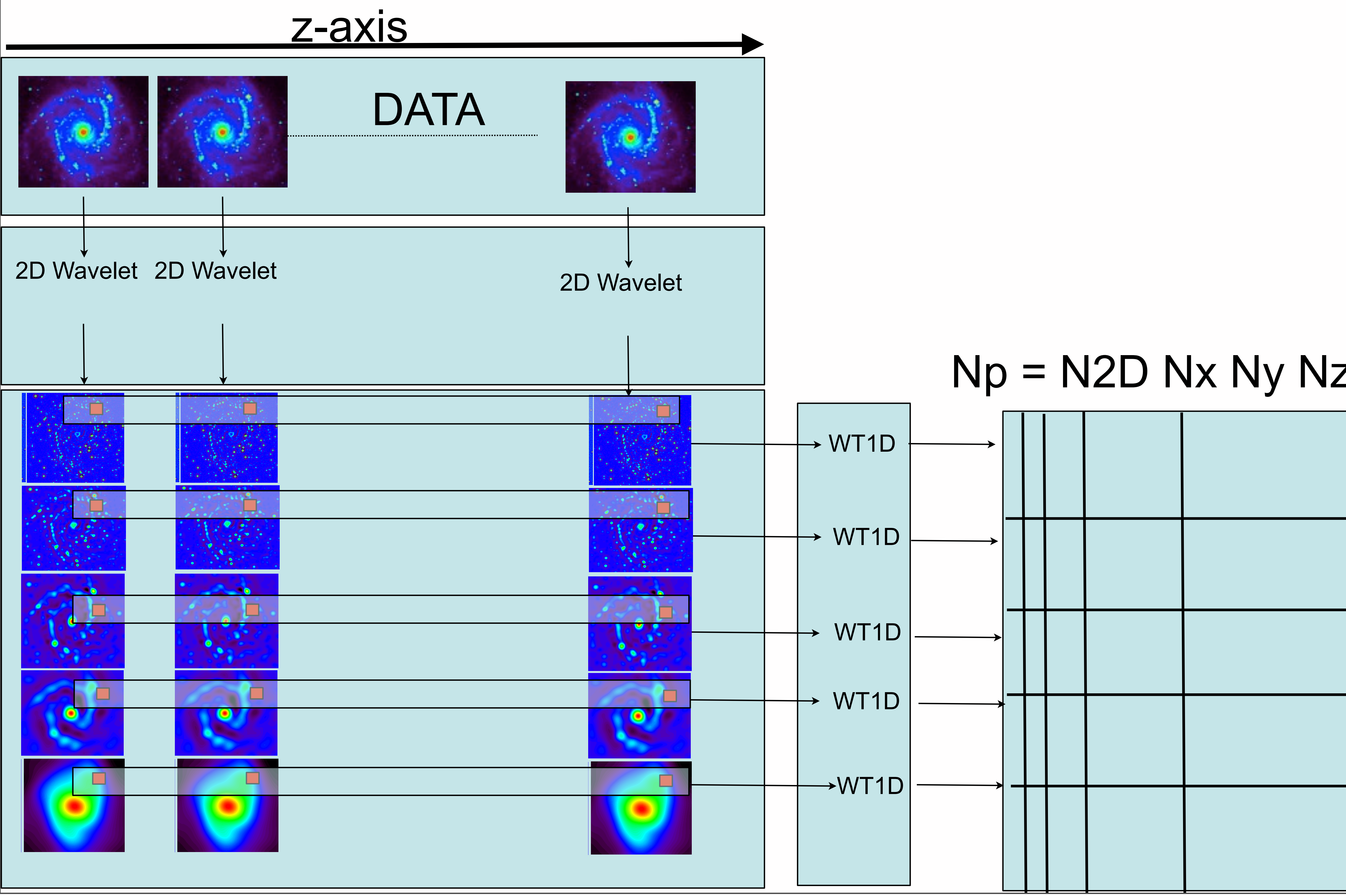

## Simulating a transient sky and a radio observation

using 32 x 32 x 64 & 128 x 128 x 64 cubes

**Sky model**

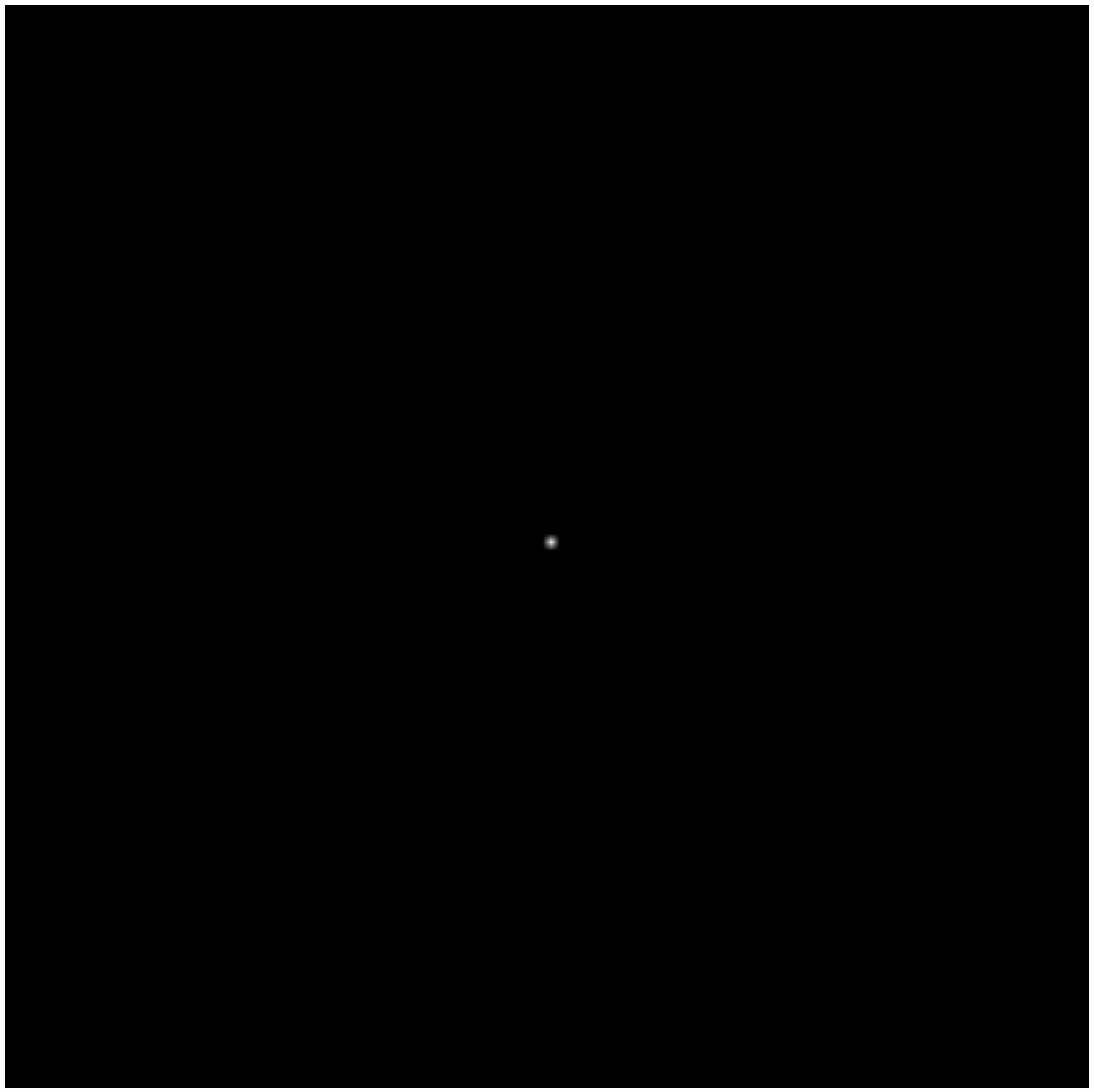

**Dirty map**

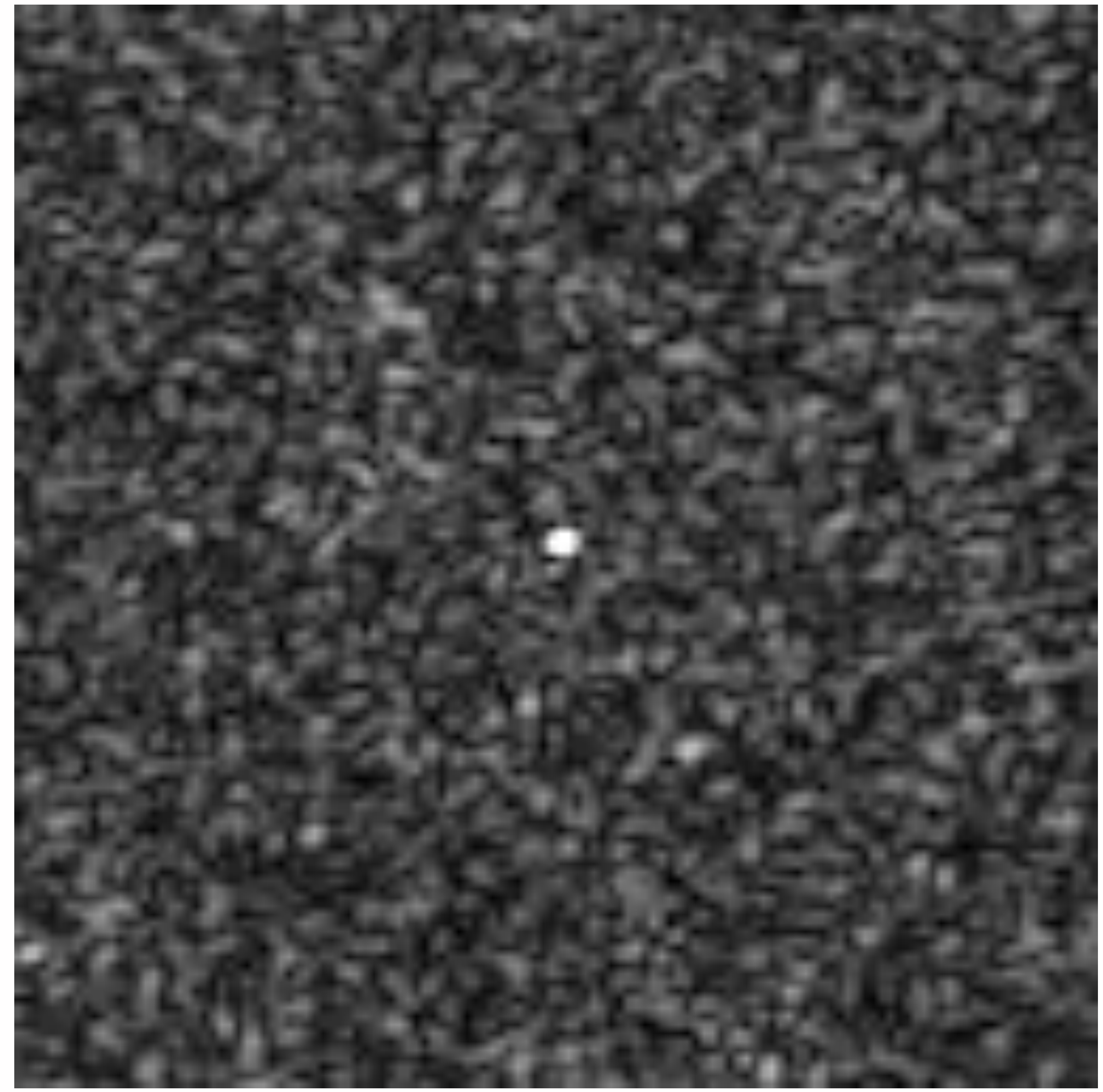

- "control" source: steady 10 FU* source
- transient gaussian source: 10 FU maximum

A new source appeared but side lobes as well !
Need a time-agile deconvolution algorithm

*FU = arbitrary flux unit

# Reconstruction

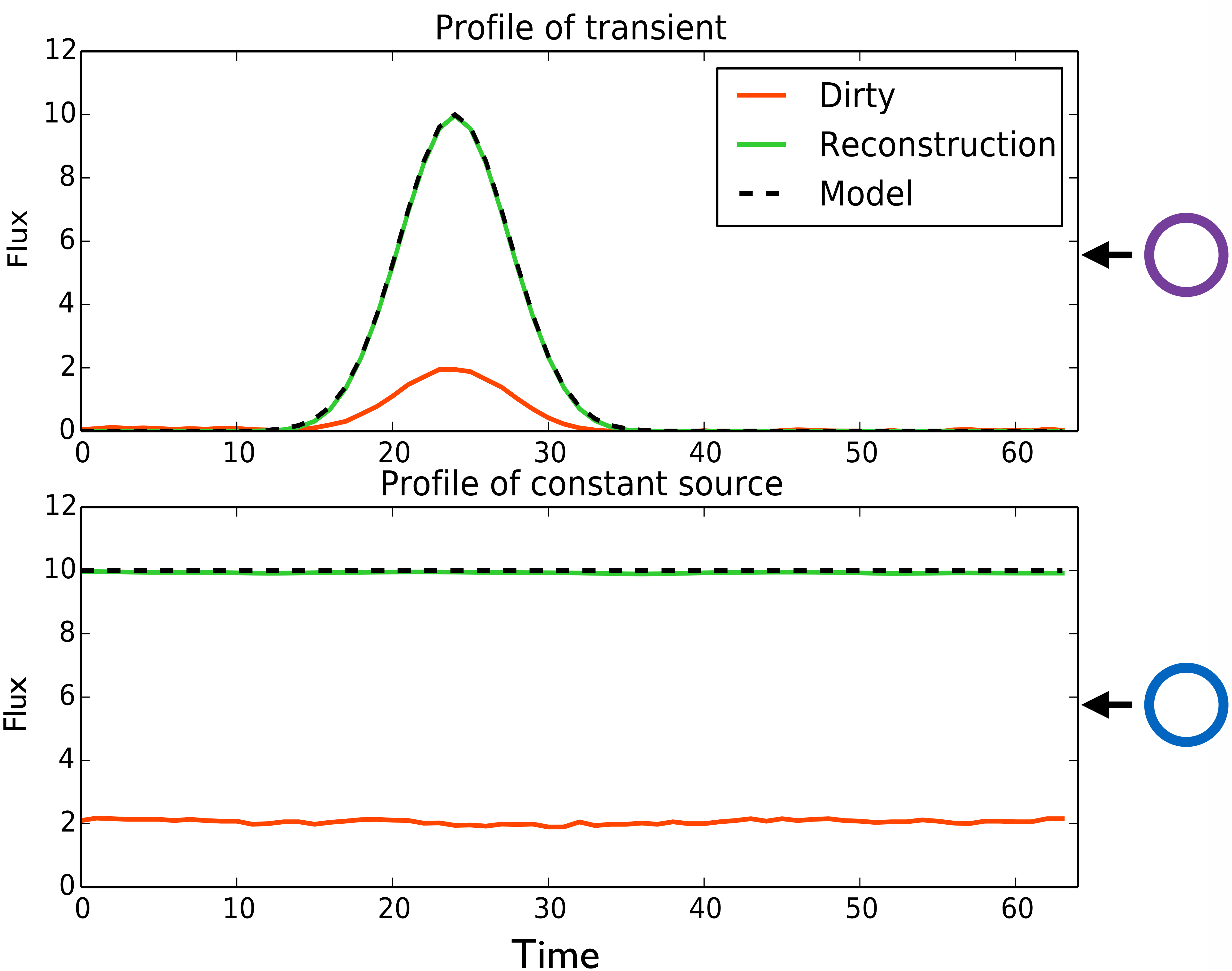


T=25

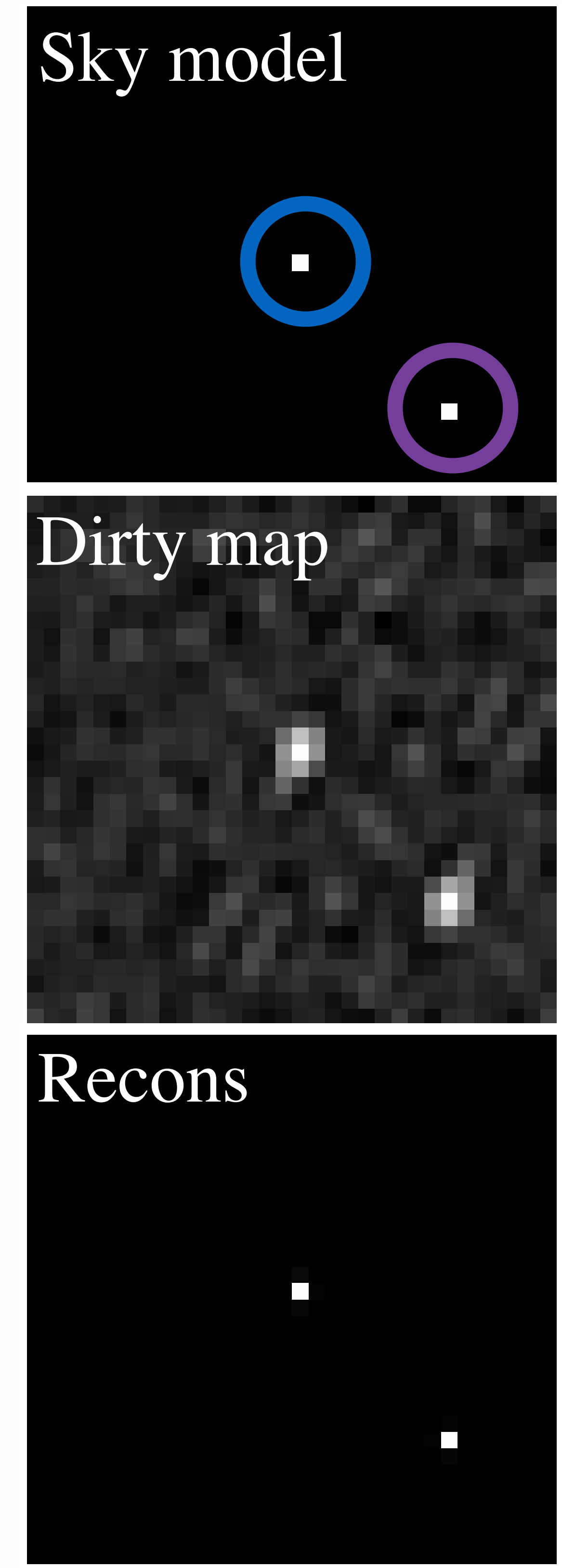


- **Accurate deconvolution with good profile match in time for the transient and the constant source**
- **Residuals down to $10^{-5}$ flux unit**

# Sparsity & Mapping



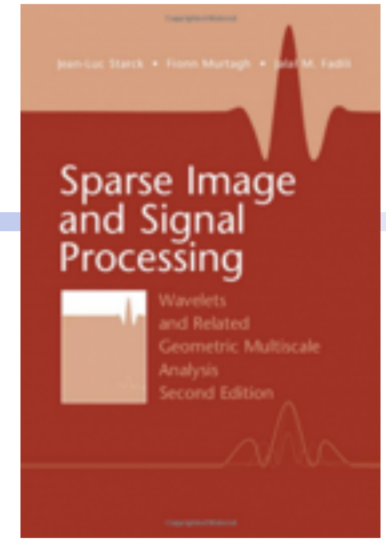


- ✓ **Sparsity is a very efficient tool to regularize inverse problems.**
- ✓ **Radio-Interferometry**
  - ➡ **2D and 3D mapping from visibilities.**
- ✓ **CMB Map Recovery:**
  - ➡ **Joint CMB map reconstruction from WMAP and Planck data**

    http://www.cosmostat.org/research/cmb/planck_wpr2/

    *J. Bobin, F. Sureau, J.-L. Starck, CMB reconstruction from the WMAP and Planck PR2 data, submitted to A&A, 2015*
- ✓ **Weak Lensing Mass Map Reconstruction**
  - ➡ **GLIMPSE2D**: A new mass mapping algorithm, based on sparsity and proximal optimization theory:

– Does not require angular binning of the ellipticities, accounts for reduced shear, and proper regularization of missing data.

=> Can include individual redshift PDFs of sources and flexion measurements if available

⇒ Can be also be used for non-parametric high-resolution cluster density mapping from weak lensing alone

**-** F. Lanusse , J.-L. Starck, A. Leonard, and S . Pires, High Resolution Weak Lensing Mass Mapping combining Shear and Flexion , submitted, **http://www.cosmostat.org/software/glimpse**

➡ **GLIMPSE3D**: Significant improvement over linear methods (Redshift bias, Smearing, Damping, Resolution).

A. Leonard, F. Lanusse, J-L. Starck, “GLIMPSE: Accurate 3D weak lensing reconstruction using sparsity”, A&A, 571, id.L1, 2014

A. Leonard, F. Lanusse, J-L. Starck, “Weak lensing reconstructions in 2D & 3D: implications for cluster studies” MNRAS, 449, 2015.